

Published in final edited form as:

Nat Metab. 2019 August ; 1(8): 790–810. doi:10.1038/s42255-019-0097-9.

Prostaglandin signals from adult germline stem cells delay somatic aging of *Caenorhabditis elegans*

Hyun Ju Lee¹, Alireza Noormohammadi¹, Seda Koyuncu¹, Giuseppe Calculli¹, Milos S. Simic², Marija Herholz¹, Aleksandra Trifunovic¹, David Vilchez¹

¹Cologne Excellence Cluster for Cellular Stress Responses in Aging-Associated Diseases (CECAD), University of Cologne, Cologne, Germany

²Department of Molecular and Cell Biology, University of California, Berkeley, Berkeley, California, USA

Abstract

A moderate reduction of body temperature can induce a remarkable lifespan extension. Here we examine the link between cold temperature, germ line fitness and organismal longevity. We show that low temperature reduces age-associated exhaustion of germ stem cells (GSCs) in *Caenorhabditis elegans*, a process modulated by thermosensory neurons. Notably, robust self-renewal of adult GSCs delays reproductive aging and is required for extended lifespan at cold temperatures. These cells release prostaglandin E2 (PGE2) to induce *cbs-1* expression in the intestine, increasing somatic production of hydrogen sulfide (H₂S), a gaseous signaling molecule that prolongs lifespan. Whereas loss of adult GSCs reduces intestinal *cbs-1* expression and cold-induced longevity, application of exogenous PGE2 rescues these phenotypes. Importantly, tissue-specific intestinal overexpression of *cbs-1* mimics cold-temperature conditions and extends longevity even at warm temperatures. Thus, our results indicate that GSCs communicate with somatic tissues to coordinate extended reproductive capacity with longevity.

Introduction

The aging process is modulated by environmental and genetic factors^{1,2}. Although extreme cold is detrimental³, a moderate reduction of body temperature induces a remarkable

Users may view, print, copy, and download text and data-mine the content in such documents, for the purposes of academic research, subject always to the full Conditions of use:http://www.nature.com/authors/editorial_policies/license.html#terms

Corresponding author: David Vilchez, PhD, Cologne Excellence Cluster for Cellular Stress Responses in Aging-Associated Diseases (CECAD), University of Cologne, Joseph Stelzmann Strasse 26, 50931 Cologne, Germany, Phone number: +49 22147884172, Fax number: +49 221 478 84045, dvilchez@uni-koeln.de.

Reporting Summary

Further information on research design is available in the Nature Research Reporting Summary linked to this article.

Author Contributions

H.J.L., A.N. and D.V. performed most of the experiments, data analysis and interpretation. S.K. assessed knockdown levels and contributed to lifespan assays and other experiments. G.C. performed some of the BrdU assays and helped with other experiments. M.S.S. generated the plasmids for tissue-specific overexpression that were used to clone *cbs-1*. M.H. performed oxygen consumption experiments. A.T. contributed with her expertise on metabolic rates and provided critical advice on the project. The manuscript was written by D.V. All the authors discussed the results and commented on the manuscript.

Competing interests

The authors declare no competing interests.

lifespan extension⁴. As such, lowering body temperature is one of the most effective interventions to extend organismal lifespan⁴. This phenomenon was first observed in poikilotherms, including *Caenorhabditis elegans*⁵⁻⁷, the fruit fly *Drosophila melanogaster*⁸, and distinct fish species^{9,10}. For instance, *C. elegans* lives shorter when shifted from the standard culturing temperature (20°C) to higher temperatures, whereas lower temperature (e.g., 15°C) extends lifespan^{7,11,12}. In mouse models, a 0.5-0.6°C reduction of core body temperature induces a 20% lifespan extension¹³. Although the longevity effects of lowering core body temperature were originally reported over a century ago¹⁴, little is known about the mechanisms underlying this process. Since temperature essentially influences every chemical and biological process, it was conventionally considered that longevity ensues from a passive thermodynamic process. In this view, cold temperature reduces the rate of chemical reactions and metabolism, resulting in slower molecular entropy, energy expenditure and pace of living. However, recent work in *C. elegans* reported that the cold-sensitive TRPA-1 channel detects low temperature during adulthood, leading to a calcium ion influx that promotes lifespan extension^{12,15}. Conversely, loss of TRPA-1 channel shortens lifespan at cold temperature, while it does not affect lifespan at warm temperature¹². Further studies identified that TRPA-1 acts in IL1 neurons, inducing neuroendocrine signaling circuits to extend longevity at cold temperature¹⁶. In addition, the co-chaperone *daf-41/p23* is also necessary for lifespan extension at low temperature¹⁷. Thus, cold-induced longevity is a regulated process that cannot be simply explained by passive changes in chemical reactions.

As temperature, fecundity is also negatively correlated with lifespan¹⁸. Among invertebrates, birds and mammals, interventions that limit investment in the germ line and reproduction induce lifespan extension¹⁸. Since tissue homeostasis and physiological integrity are constantly challenged by ever-changing metabolic, pathological and environmental conditions, evolutionary pressure has been theorized to force a re-allocation of energetic resources to prevent and repair damage to the germ line¹⁹. By this compromised distribution, the organism will ensure its reproduction, generating a healthy and fit progeny. In these lines, extensive evidence in *C. elegans* indicates that the germ line promotes somatic aging under standard and stress conditions²⁰⁻²². As such, germline-lacking worms can live up to 60% longer and exhibit increased resistance to a variety of environmental stressors, including high temperatures²⁰⁻²². Remarkably, these effects are not simply a result of sterility^{20,22}. Under standard (20°C) and warm temperatures, the germ line is responsible for the generation of signals that promote progressive deterioration of the soma and organismal aging^{20,21}. Conversely, removal of the germ line activates pro-longevity transcriptional factors in somatic tissues, resulting in lifespan extension²⁰⁻²⁴. Eventually, these transcription factors modulate downstream processes within somatic cells, such as increased autophagy or proteome stability, that contribute more directly to the longevity phenotype^{22,24-26}. Thus, these findings establish proliferating germ cells as active inhibitors of pro-longevity pathways in somatic tissues, reducing organismal lifespan.

While the impact of the germ line on lifespan at standard and warm temperatures has been extensively studied, here we examine the link between low temperature, germ line fitness and organismal longevity. Remarkably, we find that cold temperature does not extend lifespan of germline-lacking worms. Since germline-lacking worms live significantly shorter

at low temperatures when compared with wild-type worms, our results indicate that the germ line is required for cold-induced longevity. Prompted by these results, we assess whether low temperature impacts on germline aging. Indeed, low temperature ameliorates exhaustion of the germ stem cell (GSC) pool during adulthood, resulting in a delay of reproductive aging. This process is regulated by thermosensory neurons, which detect low temperatures to maintain GSC self-renewal with age. Notably, cold-induced longevity is blocked by chemical and genetic interventions that specifically diminish adult GSC proliferation. On the contrary, these interventions do not affect lifespan at higher temperatures. Robust proliferation of adult GSCs induces the expression of CBS-1 in somatic tissues such as the intestine, increasing the production of hydrogen sulfide (H₂S), a gaseous signaling molecule that extends lifespan^{27,28}. Importantly, overexpression of *cbs-1* in the intestine extends lifespan even at warm temperatures. In addition, we find that low temperature increases the production and release of prostaglandin E2 (PGE2) by GSCs, a hormone that modulates somatic tissues and promotes cold-induced longevity. Whereas loss of adult GSCs reduces somatic *cbs-1* expression and cold-induced longevity, application of exogenous PGE2 rescues these phenotypes. Taken together, our results indicate that adult GSCs communicate with somatic tissues via prostaglandin signals to extend longevity at cold temperature. This process coordinates extended reproductive capacity and long lifespan, without compromising on either the germ line or the soma.

Results

The germ line is essential for cold-induced longevity during adulthood

With the strong lifespan extension induced by lowering body temperature, we asked what role, if any, do germ cells have in this phenotype. For this purpose, we first examined *glp-1(e2141)* mutant worms, which develop into adults lacking a germ line due to a failure in germ-cell proliferation during development at the restrictive temperature (25°C)²⁹. Thus, we raised *glp-1(e2141)* mutant larvae at 25°C to obtain germline-lacking adults and shifted them to distinct temperatures. As extensively reported^{20,23}, *glp-1* germline-lacking worms were long-lived at 20°C when compared with wild-type animals under the same conditions (Fig. 1a). On the contrary, we found that *glp-1* mutants lived significantly shorter in comparison with wild-type worms at lower temperatures (*i.e.*, 15°C, 10°C) (Fig. 1a).

Although our results indicate that the pro-longevity effects of low temperature are diminished in *glp-1* germline-lacking mutants (Fig. 1b), the fact that these worms are long-lived at 20°C makes our results difficult to interpret. To further assess the impact of germline depletion in cold-induced longevity, we used *glp-4(bn2)* mutants, a distinct germline-lacking strain which has no lifespan increase relative to wild-type at 20°C^{30,31} (Fig. 1c). Notably, low temperature (15°C) did not extend lifespan of *glp-4* germline-lacking worms, as we observed in *glp-1* mutants (Fig. 1b, c). To determine whether this is a consequence of sterility per se, we assessed *fer-15(b26);fem-1(hc17)* worms that are also sterile but which still contain a proliferating germ line when raised at the restrictive temperature (25°C) during development (Supplementary Fig. 1). We found that low temperature during adulthood increased lifespan of the control sterile strain whereas it did not extend lifespan of *glp-1* germline-lacking mutants (Supplementary Fig. 2). As a result, sterile control worms

lived longer in comparison with *glp-1* mutants at low temperature (Supplementary Fig. 2). Similar to *fer-15;fem-1* worms, low temperature also extended the lifespan of distinct sterile mutants with spermatogenesis defects but which contain a proliferating germ line and generate oocytes, such as *fog-1*, *fog-2* and *spe-26* mutant worms^{32–36} (Fig. 1d, e). Thus, our results indicate that loss of cold-induced longevity is not due to sterility, but specific to depletion of the germ line. In all the above experiments, we raised both mutant and wild-type worms at the same temperature until they reached adulthood and then shifted them to the distinct temperatures to assess adult lifespan. Thus, our results suggest that the germ line is particularly important during adulthood for the cold-induced longevity phenotype. In support of this hypothesis, exposure of wild-type *C. elegans* to low temperature only during adulthood was sufficient to prolong lifespan after development at either 25°C or 20°C (Fig. 1f, g)¹⁵.

Cold temperature delays exhaustion of GSCs and reproductive aging

Prompted by our results in germline-lacking worms, we hypothesized that temperature-associated changes in the adult germ line determine cold-induced longevity. In adult *C. elegans*, the germ line is composed by a mitotic zone at the distal end followed by regions containing cells from early meiotic stages to maturing gametes, extending proximally³⁷ (Fig. 2a, b). Whereas adult germ cells are continuously lost during gametogenesis and cell death events, proliferating germ stem cells (GSCs) of the mitotic region self-renew and provide new pools of cells which enter meiosis to replenish the germ line and generate gametes³⁸. To determine the impact of temperature and age in adult germline proliferation, we raised wild-type larvae at 20°C until adulthood and then shifted them to different temperatures. Notably, the total number of germ cells within the mitotic region did not change with age or temperature (Fig. 2c and Supplementary Fig. 3). On the contrary, low temperature delayed the age-associated decline in the percentage of mitotic cells, which were labeled with bromodeoxyuridine (BrdU) (Fig. 2c, d). In addition, we observed active proliferation of germ cells for an extended fraction of the animal's mean lifespan at cold temperatures (Fig. 2e). At 25°C, the percentage of proliferating germ cells was strongly reduced (*i.e.*, less than 10% BrdU-positive cells) at day 5 whereas the organismal mean lifespan was 14 days (Fig. 2d, e). At 20°C, worms had a mean lifespan of 19.5 days with a strong decline in proliferating germ cells at day 10. However, adult worms at 15°C delayed the acute decline in proliferating germ cells until day 23, closer to their mean lifespan of 28 days. Likewise, worms at 10°C maintained a high percentage of proliferating germ cells until day 37, while their mean lifespan was 43 days (Fig. 2d, e). Thus, these results indicate that low temperature extends the ability of GSCs to self-renew during aging, sustaining the pool of proliferating cells within the mitotic region.

Besides their self-renewal ability, GSCs also produce differentiating gametes. Since more than half of the developing oocytes undergo apoptosis whereas the remaining cells progress to terminal differentiation and fertilization, GSCs are critical to replenish the pool of oocytes^{39,40}. During development, the first germ cells in hermaphrodites differentiate into spermatocytes, resulting in a limited number of 240–320 sperm, whereas subsequent germ cells generate oocytes during adulthood which can be then self-fertilized and ovulated^{32,34} (Fig. 2a). At standard temperature, *C. elegans* hermaphrodites reproduce during the first 4–5

days of adulthood and quickly exhaust their supply of self-sperm⁴¹. Likewise, worms at 15°C also self-reproduced until day 5 (Supplementary Fig. 4a). Although worms extended their self-reproductive period until day 8 of adulthood at 10°C (Supplementary Fig. 4a), the total number of eggs laid by hermaphrodites was not increased at cold temperatures (Supplementary Fig. 4b). Moreover, most of the laid eggs hatched in all the temperatures tested (Supplementary Fig. 4c). However, this period is not sufficient to assess reproductive capacity because self-progeny brood sizes are determined by the number of self-sperm⁴¹. To circumvent this limitation, 8-day adult hermaphrodites at the distinct temperatures were mated with young males for 48 h to replenish the pool of sperm. At 10°C and 15°C, worms were able to lay eggs during the following 9 and 5 days after mating, respectively (Fig. 2f). In contrast, worms at 20°C laid eggs essentially within the first 2 days after mating whereas we did not observe eggs at higher temperature. Notably, the total number of eggs laid at low temperatures was markedly higher when compared with 20°C (Fig. 2g). In addition, most of these eggs were hatched into viable larvae (Fig. 2h). Taken together, our results indicate that cold temperature sustains the GSC pool during adulthood, resulting in a higher maintenance of the proliferating germline region and reproductive capacity with age.

To assess whether maintenance of GSCs correlates with the capacity to induce cold-associated longevity, we shifted worms from higher temperature to lower temperature at different adult stages. Remarkably, cold-induced longevity was dramatically reduced when worms at 20°C were shifted to lower temperature at day 10 of adulthood (Fig. 3a), correlating with the acute decline in germline proliferation at 20°C (i.e., <10% BrdU-positive cells). Similarly, worms displayed a diminished ability to live longer under cold temperature once they reached day 5 of adulthood at 25°C (Fig. 3b), correlating with the demise of germline proliferation at this temperature (Fig. 2d). Despite the reduction in the length of cold-induced longevity, worms with low percentage of proliferating germ cells still exhibited a partial lifespan extension when shifted to cold temperature (Fig. 3a, b). In these lines, we found that shifting the worms to cold temperature after an acute decline in germline proliferation could also partially recover this phenotype (Fig. 3c).

Since somatic tissues such as thermosensory neurons detect changes in temperature^{12,16,42,43}, we asked whether these cells modulate germline maintenance at cold temperature. The cold-sensitive channel TRPA-1 senses temperature decrease in the intestine and neurons to extend lifespan^{12,15}. Concomitantly, loss of function of *trpa-1* reduces the length of cold-induced longevity^{12,15} (Fig. 3d). At early adulthood stages, lack of *trpa-1* did not affect germline proliferation under cold temperature (Fig. 3e and Supplementary Fig. 5). However, germline proliferation dramatically decreased in *trpa-1*-lacking mutants when compared with wild-type worms at older age, whereas the total number of germ cells within the mitotic region remained similar (Fig. 3e and Supplementary Fig. 5). Cold-sensitive IL1 neurons express *trpa-1*⁴⁴ and are required for the long-lived phenotype induced by low temperature¹⁶. Because transgenic expression of *trpa-1* in IL1 neurons alone is sufficient to rescue the short lifespan of *trpa-1*-lacking mutants at lower temperatures¹⁶ (Fig. 3d), we examined whether it also ameliorates the decline in germline proliferation. Indeed, specific transgenic expression of *trpa-1* in IL1 neurons rescued the defects in germline proliferation of *trpa-1* mutants at cold temperature (Fig. 3e and Supplementary Fig. 5). Since loss of *trpa-1* does not completely abolish cold-induced longevity at 15°C¹², we hypothesized that

other thermosensory neurons could also contribute to this phenotype. A pair of thermoreceptor neurons, called AFD, are required for temperature-related behaviors⁴² but do not express TRPA-1 channel⁴⁴. To assess whether AFD neurons modulate cold-induced longevity, we used worms expressing reconstituted caspase-3 under AFD-specific promoter to kill these pair of neurons⁴³. As we performed in our previous experiments with *trpa-1* mutants, we raised AFD-ablated worms at 20°C during development and then shifted them to distinct temperatures to assess adult lifespan. Notably, we found that AFD-ablated transgenic animals lived significantly shorter at cold temperature when compared with wild-type worms (Fig. 3f and Supplementary Fig. 6a). On the contrary, loss of AFD neurons did not affect lifespan at 20°C and 25°C (Supplementary Fig. 6b-c). To further assess the role of these neurons in cold-induced longevity, we examined two distinct strains carrying mutations in the *ttx-1* gene that specifically disrupt AFD structure and function^{45,46}. Both *ttx-1* mutants were short-lived when cultured at 10°C or 15°C during adulthood (Fig. 3g-h and Supplementary Fig. 7a-b). By contrast, *ttx-1* mutants had no significant lifespan change relative to wild-type at either 20°C or 25°C (Supplementary Fig. 7c-f). In both AFD-ablated and *ttx-1* mutant worms, we observed a decrease in germline proliferation under cold temperature, particularly at older age (Fig. 3i and Supplementary Fig. 8). Collectively, our results indicate that detection of low temperature by thermosensory circuits such as IL1 and AFD neurons delays GSC exhaustion.

Robust proliferation of adult GSCs determines cold-induced longevity

Our experiments with germline-lacking worms indicated that the germ line is required for cold-induced longevity. In addition, we found that low temperature maintains robust GSC proliferation during adulthood. Intrigued by these results, we asked whether there is a direct and active role of adult GSCs in cold-induced longevity. To address this hypothesis, we let worms to develop at 20°C into adults with a normal germ line and then inhibited adult GSC function by different means. In adult worms, the germ cells within the mitotic region constitute the only pool of proliferating cells in the organism⁴⁷. Thus, the treatment with 5-fluoro-2'-deoxyuridine (FUdR), an inhibitor of DNA synthesis, could particularly affect these cells in adult worms. Indeed, FUdR treatment initiated during adulthood dramatically reduced GSC proliferation at either 20°C or 15°C (Fig. 4a). Whereas FUdR treatment did not affect adult lifespan at 20°C, it blocked the lifespan extension induced by cold temperature (Fig. 4b).

To further assess the requirement for adult proliferating germ cells in cold-induced longevity, we silenced distinct regulators of GSC proliferation. First, we knocked down *mog-1*, *mog-4* and *mog-5* genes, which encode DEAH-box RNA helicases required for robust proliferation of germ cells during development⁴⁸⁻⁵⁰. When we initiated RNAi treatment in young adults after normal development of the germ line, we also observed reduced proliferation within the mitotic region (Fig. 4c, d and Supplementary Fig. 9-10). Notably, downregulation of *mog* genes during adulthood diminished the lifespan extension induced by low temperature (Fig. 4e). On the contrary, loss of *mog* expression during adulthood did not decrease lifespan at 20°C and 25°C (Fig. 4f, g). Besides *mog* genes, other RNA-binding proteins are also involved in maintenance of germline proliferation such as PGL-1, PGL-3 and GLH-1, which are all components of P-granules, a germline-specific

RNA/protein complex^{51–53}. However, the germline proliferation requirement for these specific P-granule components is sensitive to temperature. As such, their individual loss can diminish germ-cell proliferation at high temperature (25°C), but not at lower temperatures^{51–53}. Interestingly, knockdown of *pgl* genes slightly extends lifespan of wild-type worms at high temperature³⁰. In contrast to downregulation of *mog* genes, we found that knockdown of *pgl-1* alone during adulthood did not reduce germline proliferation (Fig. 4c-d) and cold-induced longevity at 15°C (Fig. 4h). Likewise, downregulation of *glh* genes did not alter the long lifespan phenotype induced by low temperature (Fig. 4h).

Although these results indicate a link between germline proliferation and cold-induced longevity during adulthood, it is important to note that *mog* genes are also expressed in somatic tissues. To circumvent potential direct effects on somatic tissues, we knocked-down the orthologues of the translational initiation factor EIF5A (*i.e.*, *iff-1*, *iff-2*), which is duplicated in *C. elegans*. Whereas *iff-2* is only expressed in somatic tissues⁵⁴, *iff-1* is specifically expressed in the germ line and, particularly, abundant in the distal gonad where mitotic divisions occur⁵⁴. In fact, *iff-1* is essential for germline proliferation at either larvae or adult stages^{54,55}. As such, *iff-1* RNAi initiated during adulthood was sufficient to decrease the proliferation of germ cells in the distal gonad (Fig. 4c, d and Supplementary Fig. 9). Notably, knockdown of *iff-1* during adulthood diminished lifespan extension induced by low temperatures (Fig. 4i, j), but did not shorten lifespan at higher temperatures (*i.e.*, 20°C and 25°C) (Fig. 4k, l). On the contrary, loss of *iff-2* during adulthood did not impair germline proliferation (Fig. 4c, d) and cold-induced longevity (Fig. 4i, j). Upon knockdown of *eif-2A*, a different translational initiation factor, worms also exhibited a normal proliferating germ line (Fig. 4c, d) and extended lifespan when compared with control worms at cold temperature (Fig. 4k, l). Altogether, our data suggest that maintenance of adult GSC proliferation determines cold-induced longevity.

Prompted by these results, we assessed how temperature impinges on *iff-1* mutants, which develop into young adult worms with very few germ cells (~40 germ nuclei) when compared with controls (~2000 germ nuclei)⁵⁴, resembling *glp-1* mutants. As *glp-1* worms (Fig. 1b), *iff-1* germline-less mutants were also long-lived at 20°C while they lived shorter than the wild-type strain at 15°C (Supplementary Fig. 11a, b). Although ablation of the germ line from development in either *iff-1* or *glp-1* mutants cannot be directly equated to the impairment of GSC proliferation induced by *iff-1* RNAi at the adult stage, these results further support a role of the germ line in cold-induced longevity. In these lines, *iff-1* knockdown during adulthood did not further decrease the lifespan of distinct germline-lacking strains at cold temperature (Supplementary Fig. 12a, b). As a more formal test of the specific role of adult GSCs, we knock-downed *iff-1* in adult sterile worms with a proliferating germline and found a decrease in cold-induced longevity (Supplementary Fig. 12c). These results not only strengthened the link between adult GSCs and cold-induced longevity, but also indicate that sterility does not affect the long lifespan phenotype. Indeed, knockdown of *iff-1* during adulthood reduces GSC proliferation and cold-induced longevity (Fig. 4d, j), but did not strongly affect the number of eggs laid by self-fertilizing hermaphrodites (Supplementary Fig. 13a, b). Because maintenance of germline proliferation is required for cold-induced longevity, we asked whether an over-proliferative germ line could further extend lifespan at low temperature. Mutations in *gld-1*, a tumor-suppressor

factor, promote that germ cells reenter the mitotic cycle and overproliferate⁵⁶. Likewise, knockdown of *gld-1* also induces over-proliferation of the germ line⁵⁷. Eventually, these over-proliferating germ cells break out of the gonad and fill the animal's body, killing the worms at early adulthood stages. Concomitantly, these worms exhibit a short lifespan at 20°C⁵⁸ (Supplementary Fig. 14a). Similarly, both tumorous *gld-1* mutations and *gld-1* knockdown from either development or adulthood also killed *C. elegans* early in life at lower temperature (Supplementary Fig. 14b). Collectively, our data indicate that cold-induced longevity is determined by an extended maintenance of the physiological pool of proliferating GSCs, while abnormal over-proliferation of these cells is deleterious for the animal.

Adult proliferating germ cells induce *cbs-1* in the intestine to extend lifespan

Since our results suggest a direct regulation of cold-induced longevity by adult GSCs, we asked whether these cells regulate somatic tissues to prolong lifespan. Whereas low temperature slightly increased motility, we did not observe defects in germline-lacking mutant worms when compared with either wild-type or *fer-15;fem-1* control sterile worms (Supplementary Fig. 15a). Likewise, inhibition of adult germline proliferation upon *iff-1* or *mog-5* RNAi treatment did not affect motility at cold temperature (Supplementary Fig. 15b). We also examined body size and found that neither germline ablation nor inhibition of adult germline proliferation have a notable effect on the animal's size (Supplementary Fig. 15c-f). In *C. elegans*, metabolic rates increase with temperature and are often negatively correlated with longevity⁵⁹. As indicated by lower oxygen consumption, long lifespan of wild-type worms was accompanied by reduced metabolic rates at 15°C (Supplementary Fig. 16a). However, metabolic rates increased in *fer-15;fem-1* sterile worms at cold temperature (Supplementary Fig. 16a), despite they exhibited a cold-induced longevity phenotype (Fig. 1d). In *glp-1* germline-lacking mutants, we did not find significant changes in metabolic rates when they were shifted to 15°C (Supplementary Fig. 16a). More importantly, the short lifespan of *iff-1* RNAi-treated worms did not correlate with increased metabolic rates at 15°C (Supplementary Fig. 16b). In fact, *iff-1* RNAi-treated worms had a decrease in metabolic rates compared with control worms, resembling *iff-2* RNAi treatment which does not affect cold-induced longevity (Supplementary Fig. 16b). Thus, inhibition of adult GSC proliferation did not have a strong effect on features such as motility, body size or metabolic rates, indicating that these cells regulate cold-induced longevity by distinct mechanisms.

To gain further insights into somatic changes induced by GSCs at low temperature, we used a quantitative proteomics approach. We identified 225 up-regulated and 233 down-regulated proteins at 20°C when compared with *C. elegans* cultured at 15°C (Supplementary Data 1). We hypothesized that inhibition of germ-cell proliferation during adulthood at 15°C triggers similar changes in lifespan regulators to those induced by temperature increase. Thus, we examined the proteome of *iff-1* RNAi-treated worms at cold temperature (Supplementary Data 1). Besides IFF-1 levels, quantitative proteomics analysis revealed that other 152 proteins are significantly changed upon *iff-1* knockdown during adulthood at 15°C (Supplementary Data 1). Among them, 27 proteins were also up-regulated at 20°C (Fig. 5a, Supplementary Fig. 17 and Supplementary Data 1). Likewise, 27 proteins were downregulated in both *iff-1* RNAi and 20°C conditions (Fig. 5a, Supplementary Fig. 17 and

Supplementary Data 1). To examine whether these proteins modulate longevity at cold temperatures, we performed a RNAi screen (Supplementary Table 1). Notably, knockdown of several genes reduced cold-induced longevity as we further validated in independent experiments (Fig. 5b-e). In particular, genes encoding proteins which are increased at cold-temperature and down-regulated by loss of *iff-1* (Fig. 5a). The strongest effect was induced by knockdown of distinct subunits (*cct-2*, *cct-5*, *cct-6*) of the chaperonin TRiC/CCT complex (Fig. 5b). Since loss of a single subunit is sufficient to impair the assembly of the complex²⁵, our results suggest that increased TRiC/CCT assembly is required for cold-induced longevity. Indeed, knockdown of a different *cct* subunit (*cct-8*) also shortened lifespan at 15°C (Supplementary Fig. 18). Besides *cct* subunits, loss of either the hsp70 chaperone *hsp-1* or the RNA polymerase II *ama-1* reduced lifespan extension at cold temperature (Fig. 5c, d). Likewise, up-regulated levels of CBS-1, the orthologue of human cystathionine β -synthase (CBS)^{27,60}, were required for the full extent of the longevity phenotype at 15°C (Fig. 5e). At lower temperature (10°C), knockdown of *cct* subunits, *hsp-1*, *ama-1* and *cbs-1* also induced a decrease in the longevity phenotype (Fig. 5f). On the contrary, knockdown of these genes did not shorten lifespan at higher temperatures (20°C and 25°C) (Fig. 5g, h). Whereas these factors regulated cold-induced longevity in wild-type worms with a proliferating germ line, their knockdown did not further decrease the short lifespan of germline-lacking worms at 15°C (Supplementary Fig. 19). Taken together, our results indicate a requirement for high expression of *cct* subunits, *hsp-1*, *ama-1*, and *cbs-1* in the cold-induced longevity mediated by proliferating germ cells.

Prompted by these results, we asked how these factors impinge upon cold-induced longevity. For instance, they could modulate longevity by directly affecting germ-cell proliferation. Another intriguing possibility is that proliferating germ cells induce specific factors in somatic tissues, resulting in lifespan extension. To define the factors that fall into each category, we first assessed their effects on germline proliferation (Fig. 6a-b and Supplementary Fig. 20). Loss of *cct* subunits dramatically decreased the number of proliferating germ cells in wild-type worms (Fig. 6a, b). In these lines, tissue-specific knockdown in the germ line alone reduced cold-induced longevity (Supplementary Fig. 21a). Remarkably, tissue-specific knockdown in either neurons or intestine also partially diminished the longevity phenotype (Supplementary Fig. 21b-e). Thus, *cct* subunits could act in both the germ line and the soma to prolong lifespan at low temperature. Besides *cct* subunits, loss of *ama-1* also resulted in a strong decrease of germline proliferation (Fig. 6a, b). Whereas knockdown of *ama-1* in the intestine alone did not affect lifespan, we found a reduction of cold-induced longevity when the RNAi was also efficient in the germ line (Supplementary Fig. 22). In addition, tissue-specific knockdown of *ama-1* in neurons also slightly decreased cold-induced longevity (Supplementary Fig. 22). In comparison with *cct* subunits or *ama-1*, loss of *hsp-1* slightly decreased germline proliferation (Fig. 6a, b), indicating an important role in somatic tissues. Indeed, neuron-specific knockdown of *hsp-1* dramatically shortened longevity at cold temperature, whereas its loss in either muscle or intestine did not significantly affect lifespan (Supplementary Fig. 23a-c). However, knockdown of *hsp-1* in the germ line alone also decreased cold-induced longevity (Supplementary Fig. 23d, e). Thus, although *cct* subunits and *hsp-1* could act in somatic tissues to extend lifespan, their direct effects in germ-cell proliferation also modulate

organismal longevity. For this reason, we focused on *cbs-1*, the only regulator of cold-induced longevity that did not affect the number of proliferating germ cells (Fig. 6a, b). Whereas specific knockdown of *cbs-1* in neurons did not change lifespan, its downregulation in either the muscle or intestine significantly shortened cold-induced longevity (Fig. 6c-e). Notably, longevity was not further reduced when the germ line also responded to RNAi treatment (Fig. 6f, g). In addition, we found that knockdown of *cbs-1* in the germ line alone does not impair cold-induced longevity (Fig. 6h).

Altogether, our results suggest that proliferating germ cells induce *cbs-1* in specific somatic tissues to extend longevity at cold temperature. To assess this hypothesis, we generated a transcriptional reporter construct. At 20°C and 25°C, *cbs-1* was mostly expressed in the posterior intestine (Fig. 7a). At cold temperatures, *cbs-1* expression increased particularly in the intestine and also the body muscle (Fig. 7a, b). Notably, FUdR treatment reduced the high expression of *cbs-1* in somatic tissues induced by cold temperature (Fig. 7a, b). Likewise, knockdown of either *iff-1* or *mog-5* decreased somatic expression of *cbs-1* at cold temperature (Fig. 7c, d). Importantly, we found that somatic expression of *cbs-1* was also downregulated when we specifically knocked-down these factors in the germ line alone (Supplementary Fig. 24a, b). Thus, our results indicate that proliferating germ cells regulate cold-associated induction of *cbs-1* in somatic tissues such as the intestine.

With the strong connection between germ line, cold-induced longevity and up-regulation of somatic expression of *cbs-1*, we assessed whether intestinal overexpression of *cbs-1* can rescue the short lifespan of germline-lacking worms at cold temperature. Whereas tissue-specific overexpression of *cbs-1* in the intestine did not further increase cold-induced longevity of wild-type worms, it extended the short lifespan of *glp-1* germline-lacking mutants (Supplementary Fig. 25a). In addition, intestinal overexpression of *cbs-1* also partially rescued the short lifespan of worms with defects in adult germline proliferation induced by FUdR treatment at low temperature (Supplementary Fig. 25b). Collectively, our data suggest that intestinal up-regulation of *cbs-1* modulated by GSC proliferation contributes to cold-induced longevity.

CBS is a key enzyme of the transsulfuration pathway that mediates the interconversion of cysteine and homocysteine. CBS activity produces cystathionine and hydrogen sulfide (H₂S)^{27,60}, which acts as a gaseous signaling molecule that reduces blood pressure⁶¹ and prevents neurodegeneration in mammals⁶². In addition, dietary restriction induces high levels of H₂S that contribute to lifespan extension phenotype in yeast, worm, fruit fly and rodents²⁷. Importantly, exogenous addition of H₂S is sufficient to extend lifespan of *C. elegans*²⁸. Since up-regulated levels of *cbs-1* contributed to cold-induced longevity, we examined H₂S amounts. Notably, low temperatures increased H₂S gas levels (Fig. 7e). Knockdown of *cbs-1* diminished the production of H₂S at cold temperature whereas its overexpression increased H₂S levels (Fig. 7f, g). Moreover, inhibition of germline proliferation by knockdown of either *iff-1* or *mog-5* was sufficient to decrease H₂S production at 15°C, providing a link between H₂S levels and the cold-induced longevity modulated by adult GSCs (Fig. 7h).

As shown above, tissue-specific overexpression of *cbs-1* in the intestine alone did not further extend longevity of worms with endogenous high levels of this protein at cold temperature

(Supplementary Fig. 25, 26). Likewise, ubiquitous somatic overexpression of *cbs-1* did not significantly increase cold-induced longevity (Supplementary Fig. 26). Thus, we asked how somatic overexpression of *cbs-1* affects lifespan at higher temperatures when worms have lower endogenous levels of *cbs-1*. Ubiquitous somatic overexpression of *cbs-1* extends lifespan at 20°C²⁷ (Fig. 7i). Notably, we found that ubiquitous somatic up-regulation of *cbs-1* induced longevity even at warm temperature (25°C) (Fig. 7j). Although tissue-specific overexpression in the muscle or neurons also extended longevity, we observed the strongest effects upon intestinal overexpression of *cbs-1* at both 20°C and 25°C (Fig. 7k, l). Thus, up-regulation of *cbs-1* in the intestine could mimic low temperature conditions and prolong lifespan. Altogether, our results suggest that adult proliferating germ cells induce *cbs-1* expression in somatic tissues such as the intestine, a process that contributes to cold-induced longevity.

Release of prostaglandin E2 by GSCs promotes longevity at cold temperatures

To assess the mechanism by which adult germ cells induce *cbs-1* expression in the intestine at cold temperature, we performed transcriptome analysis of extruded germ lines from wild-type worms upon *iff-1* knockdown or temperature increase (Supplementary Data 2). When compared with the germ line of nematodes cultured at 15°C, we found 248 up-regulated transcripts and 433 down-regulated transcripts in the germ line of both *iff-1* RNAi-treated worms and 20°C-cultured worms (Supplementary Fig. 27a and Supplementary Data 2). Among these common down-regulated transcripts, we did not observe decreased expression of signaling peptides (*i.e.*, nlp, flp or insulin-like peptides) or genes involved in the synthesis of sex steroid hormones (*e.g.*, pregnenolone) (Supplementary Data 2). However, the expression of *pges-2*, the worm orthologue of human *PTGES2*, was down-regulated in the germ line by either *iff-1* knockdown or temperature increase (Supplementary Fig. 27b and Supplementary Data 2). *PTGES2* encodes a membrane-associated prostaglandin E synthase, which catalyzes the conversion of prostaglandin H2 into the more stable prostaglandin E2 (PGE2)⁶³. Notably, we found that low temperature increases the levels of PGE2 (Fig. 8a). By western blot, we confirmed that worms exhibit higher protein levels of PGES-2 at cold temperature (Fig. 8b). Immunohistochemistry experiments indicated that PGES-2 is highly expressed in the germ line compared to the intestine (Fig. 8c). Strikingly, low temperature promoted the enrichment of PGES-2 in the plasma membrane of germ cells whereas this enzyme was essentially concentrated in the nucleus at higher temperature (Fig. 8c). Prompted by these results, we examined a potential link between *pges-2* and cold-induced longevity. Notably, *pges-2* mutant animals lived significantly shorter when compared with wild-type worms at cold temperatures (Fig. 8d and Supplementary Fig. 28). However, they did not exhibit decreased lifespan at 20°C or 25°C (Fig. 8d and Supplementary Fig. 28). Moreover, we found that *pges-2* mutant worms exhibit a significant decline in somatic expression of *cbs-1* at cold temperature when compared with wild-type worms (Fig. 8e, f). In contrast, *pges-2* mutation did not further decrease the low *cbs-1* expression of worms at 20°C (Fig. 8e, f). To further assess whether the prostaglandin E synthase activity of *pges-2* is necessary for cold-induced longevity, we added exogenous PGE2 hormone. Indeed, PGE2 rescued the low somatic expression of *cbs-1* in *pges-2* mutants and extended their short lifespan at cold temperature (Fig. 8g-i). Recently, a study reported that the co-chaperone *daf-41/p23* shortens lifespan at warm temperature, whereas it is necessary for the long

lifespan induced by cold temperature¹⁷. Importantly, epistasis experiments showed that the co-chaperone activity of *daf-41/p23* is involved in lifespan regulation at warm temperature, but not cold temperature¹⁷. Thus, *daf-41/p23* may modulate cold-induced longevity through a different pathway, although the detailed mechanism is not entirely understood. Besides its co-chaperone activity, p23 also exhibits prostaglandin E2 synthase activity *in vitro*⁶⁴. Although experiments in mouse models failed to support a function of p23 in PGE2 biosynthesis⁶⁵, we asked whether the potential PGE2 synthase activity of *daf-41/p23* modulates the effects of the germ line in cold-induced longevity. We found that ubiquitous and germline-specific knockdown of *daf-41/p23* did not diminish the somatic up-regulation of *cbs-1* induced by cold temperature (Supplementary Fig. 29a-d). In addition, knockdown of *daf-41/p23* in the germ line alone did not shorten longevity at cold temperature (Supplementary Fig. 29e). Taken together, our results support an important role of *pges-2* in the germ line to modulate cold-induced longevity, whereas *daf-41/p23* is dispensable in this tissue for the long lifespan phenotype.

Since *pges-2* mutants had normal numbers of proliferating germ cells (Supplementary Fig. 30), our results indicate that *pges-2* activity in the germ line modulates cold-induced longevity by influencing somatic tissues rather than directly affecting germ cell proliferation. The release of prostaglandin from cells is mediated by a specific transporter, ABCC4 (ATP binding cassette subfamily C member 4)⁶⁶. Knockdown of *mip-6*, the worm orthologue of ABCC4, diminished cold-induced longevity (Fig. 8j). In contrast, loss of *mip-6* did not shorten lifespan of worms at 20°C (Fig. 8j). Whereas exogenous PGE2 hormone did not further extend cold-induced longevity of control worms, it rescued the short lifespan phenotype of *mip-6* RNAi-treated worms at cold temperature (Fig. 8k). Tissue-specific knockdown of *mip-6* in either the intestine or neurons did not affect longevity at cold temperature (Fig. 8l, m). Importantly, we found a decline in cold-induced longevity when the RNAi was efficient in the germ line (Fig. 8n and Supplementary Fig. 31). Thus, these results suggest that the release of PGE2 by the germ line regulates cold-induced longevity. To test this hypothesis, we inhibited adult GSC proliferation by FUdR treatment and examined intestinal *cbs-1* expression upon application of exogenous PGE2 hormone. Remarkably, exogenous PGE2 was sufficient to rescue the low expression of intestinal *cbs-1* induced by FUdR treatment (Fig. 9a, b). Likewise, PGE2 rescued the decline in cold-induced longevity induced by loss of GSC proliferation (Fig. 9c). In addition, exogenous PGE2 extended the short lifespan phenotype of *gfp-1* germline-lacking worms at cold temperature (Supplementary Fig. 32). Altogether, our data indicate that the germ line communicates with somatic tissues via PGE2 signals to extend longevity at cold temperature (Fig. 9d).

Discussion

The aging process is regulated by a complex network of interconnected cell non-autonomous events, as distinct tissues can influence the aging of distal organs⁶⁷. In this intricate system, the germ line has a central role in the regulation of somatic aging⁶⁸. Particularly, previous studies found that the germ line can actively promote the deterioration of the soma during the aging process^{20,68}. Since food sources can be largely unpredictable and insufficient in nature, and the integrity of tissues is constantly challenged by environmental or metabolic

conditions, this system may facilitate a compromised distribution of limited resources to protect the germ line ensuring the fitness of the progeny in line with the disposable soma theory of aging. However, here we find an unexpected role of the germ line in the long lifespan phenotype induced by cold temperature. Notably, low temperature does not extend lifespan in germline-lacking mutants, providing a first indication that this tissue is required for cold-induced longevity. Ablation of the germ line from development could induce numerous changes, but our results indicate that this tissue is particularly required during adulthood for cold-induced longevity. Intrigued by these results, we examined whether temperature-associated changes determine the fitness of the adult germ line and how these changes impinge on cold-induced longevity. Besides its effects on lifespan, we find that low temperature also slows down reproductive aging. This process ensues from a delay in the age-associated exhaustion of adult GSCs, resulting in extended reproductive capacity. Notably, maintenance of GSC function is determined by the TRAP-1 channel, which acts in IL1 neurons to detect low temperature. Besides IL1 neurons, we find that dysregulation of thermosensory AFD neurons also shortens lifespan and germline proliferation at cold temperatures, but it does not reduce lifespan at standard or warm temperatures. Since AFD neurons do not express TRPA-1 channel⁴⁴, it will be fascinating to examine how these cells sense and process low temperature to communicate with the germ line. We speculate that AFD neurons constitutively release a pro-longevity signal when they are inactive or at a low activity state under cold temperature conditions. Conversely, AFD activation by temperature increase may prevent the release of this pro-longevity factor. Besides their effects at cold temperature, AFD neurons also induce heat shock response under heat stress conditions (>30°C)⁶⁹. Although we did not observe effects of AFD neurons in lifespan at moderately warm temperature (25°C), other studies reported that ablation of these neurons can reduce survival at 25°C¹¹. In our experiments, worms were maintained and raised at 20°C during development before shifting them to distinct temperatures to assess adult lifespan. In contrast, worms were cultured in the aforementioned study at a given experimental temperature for at least two generations before adult lifespan analysis at this specific temperature. Moreover, they performed lifespan experiments on FUdR to inhibit progeny, while we avoided this treatment given its effects on germline proliferation. Although it is difficult to directly compare both studies because the divergent experimental conditions, these differences raise the intriguing possibility that adaptation to temperature and other conditions can also influence how AFD neurons process temperature signals to modulate lifespan.

Whereas our data indicate that somatic tissues such as IL1 and AFD neurons detect and process temperature changes to delay GSC exhaustion, we find that these cells, in turn, promote somatic fitness of distal tissues and organismal longevity at low temperatures. To assess the requirement for adult GSCs in cold-induced longevity, we first treated adult worms with FUdR, which is extensively used to inhibit progeny at standard temperatures because it does not affect longevity of wild-type worms under these conditions^{5,70–72}. We find that FUdR inhibits GSC proliferation at both 20°C and 15°C, but this demise of adult GSCs only shortens lifespan at cold temperature. However, caution is needed to interpret these results. Besides its effects on germline proliferation, FUdR treatment also improves proteostasis⁷³. In addition, FUdR affects bacterial ribonucleotide metabolism and has

different effects depending on the *E. coli* strain used to feed the worms, modulating host-microbiome co-metabolism in *C. elegans*⁷⁴. For this reason, we validated our results by RNAi of modulators of GSC proliferation during adulthood. For instance, we knocked down the expression of *iff-1*, a regulator of germline proliferation which is only expressed in this tissue⁵⁴. Loss of *iff-1* during adulthood blocks cold-induced longevity, without reducing lifespan at warmer temperatures. Importantly, knockdown of *iff-1* does not affect fertility in early adult stages while it has a strong effect in GSC proliferation at later stages, supporting a specific signaling role of adult GSCs in cold-induced longevity.

We then identify that robust proliferation of GSCs up-regulates proteostasis components (e.g., *cct* subunits and *hsp-1*) as well as pro-longevity factors such as H₂S. This signaling gaseous molecule is produced by *cbs-1*, which expression is induced in somatic tissues such as the intestine by adult GSCs at low temperatures. Notably, intestinal *cbs-1* overexpression is sufficient to extend longevity even at warm temperatures, mimicking cold-temperature conditions. It is important to note that intestinal *cbs-1* overexpression does not completely rescue the pronounced short-lived phenotype of worms with defects in adult germline proliferation. This partial rescue upon intestinal *cbs-1* overexpression could be explained by different possibilities. Besides its effects in the intestine, cold temperature also triggers *cbs-1* expression in the muscle. Conversely, muscle-specific knockdown of *cbs-1* decreases cold-induced longevity. Therefore, up-regulation of *cbs-1* in the muscle could contribute to cold-induced longevity. In addition, our results indicate that *cbs-1* is not the only factor involved in cold-induced longevity and up-regulation of other factors can also contribute to this phenotype. For instance, loss of *cct* subunits in the intestine and neurons as well as knockdown of *hsp-1* in neurons diminish cold-induced longevity.

Interestingly, it has been reported that *glp-1* germline-lacking mutant worms also exhibit increased levels of *cct* subunits and H₂S production in somatic tissues at standard and warm temperatures, contributing to lifespan extension under these conditions^{25,75}. Thus, a fascinating possibility is that germ cells can either promote or inhibit the same downstream pathways in somatic tissues depending on the environmental and physiological conditions. In addition, depletion of the germ line from development could induced additional physiological changes when compared to inhibition of GSC proliferation after the adult germ line is formed. Our experiments in germline-lacking models were a first indication of a potential role of the germ line in cold-induced longevity, as we further validated by rescue experiments overexpressing *cbs-1* in the intestine of these worms. However, absence of the germ line cannot be directly equated with reduced adult GSC proliferation. In these lines, we observe that both *iff-1* or *glp-1* germline-lacking mutants are long-lived at 20°C, whereas *iff-1* RNAi in adult wild-type worms does not extend lifespan at this temperature.

Little is known about the specific signaling molecules by which the germ line communicates with somatic tissues. At cold temperature, our findings establish a role of PGE2 release by adult GSCs in extended longevity. Thus, this hormone could be an important determinant of long lifespan under specific conditions such as low temperature. Prostaglandins are lipid compounds derived from arachidonic acid. Interestingly, administration of arachidonic acid increases resistance of *C. elegans* to starvation and extends life span in conditions of food abundance⁷⁶. It is important to note that alterations in the synthesis or release of PGE2 do

not completely block cold-induced longevity. Therefore, other signaling pathways could also contribute to modulation of somatic tissues by germ cells at cold temperature.

Taken together, our results suggest a cell non-autonomous mechanism (i.e., neurons-germline-intestine axis) that coordinates extended reproductive capacity with long lifespan under cold temperature, without the need of sacrificing either the germ line or the soma. Since it is generally considered that the germ line and fertility induce somatic aging, this unexpected pro-longevity role of adult GSCs have important implications for the understanding of the aging process. Indeed, our results raise the intriguing possibility that germ cells activate distinct signals to differentially modulate somatic tissues depending on the physiological and environmental conditions. This could be of particular interest for our ever-aging society, because several studies indicate that women who have later menopause tend to live longer as well as reduced risk of cardiovascular disease and less loss of bone density^{77–79}. An intriguing question is why the germ line promotes longevity at cold temperature. In contrast to high temperatures, low temperature reduces the rate of chemical reactions and molecular entropy, a process that may decrease the damage and deterioration of distinct tissues triggered by cellular metabolism. Concomitantly, this process could ameliorate the pressure to prevent and repair damage to tissues. We speculate that these conditions facilitate the distribution of resources, reducing the need to compromise on either the soma or the germ line. Cold temperatures are detected by thermosensory neurons that delay exhaustion of GSCs, resulting in the ability to reproduce at older ages. Since this process may also require a healthy soma, we speculate that GSCs actively communicate with other tissues such as the intestine to ensure the fitness of the organism and the ability to reproduce for extended periods of time.

Methods

C. *elegans* strains and maintenance

C. elegans strains were grown and maintained on standard Nematode Growth Medium (NGM) seeded with *E. coli* (OP50)⁸⁰. Wild-type (N2), CB4037 (*glp-1(e2141)III*), SS104 (*glp-4(bn2)I*), CF512 (*fer-15(b26)II;fem-1(hc17)IV*) (*fer-15* is also named *rff-3*), TQ233 (*trpa-1(ok999)IV*), GN112 (p[*Is2*][*gcy-8p::TU#813* + *gcy-8p::TU#814* + *unc-122p::GFP* + *gcy-8p::mCherry* + *gcy-8p::GFP* + *ttx-3p::GFP*]), JN215 (*iff-1(tm483)III/hT2* [*bli-4(e937)* let-?(*q782*) q[*Is48*](*I;III*)]), PR767 (*ttx-1(p767)N*), PY1283 (*ttx-1(oy29)* oy[*Is17*] [*gcy-8p::GFP* + *lin-15(+)*]V), BA837 (*spe-26(it112)IV*), CB4108 (*fog-2(q71)N*), JK560 (*fog-1(q250)I*) and JK1466 (*gld-1(q485)dpy-5(e61)unc-13(e51)I*) were provided by the *Caenorhabditis* Genetics Center (CGC) (University of Minnesota), which is supported by the NIH Office of Research Infrastructure Programs (P40 OD010440). CF2424 (PR767 (*ttx-1(p767)N*) outcrossed 4 times to wild-type N2) was provided by S.J. Lee (Korea Advanced Institute of Science and Technology, South Korea). AA1724 (*pges-2(ok3316)IV*) was provided by A. Antebi (Max Planck Institute for Biology of Ageing, Germany) and was generated by outcrossing the RB2421 strain (*pges-2(ok3316)IV*) 4 times to wild-type N2. RB2421 was made by the *C. elegans* Gene Knockout Project at the Oklahoma Medical Research Foundation. TQ6891 (*xuEx1670[aqp-6p::trpa-1::sl2::yfp]; trpa-1(ok999)IV*) was a kind gift from X.Z. Shawn Xu (University of Michigan, USA).

For tissue-specific RNAi experiments, we used either *rde-1* or *sid-1* mutant animals in which wild-type *rde-1* or *sid-1* genes have been rescued using tissue-specific promoters, respectively. Tissue-specific knockdown was confirmed in the original publications. In WM118 strain (*rde-1(ne300)V*; neIs9[*myo-3p::HA::RDE-1* + *rol-6(su1006)*], RNAi treatment is only effective in muscle⁸¹. In VP303 strain (*rde-1(ne219)V*; kbIs7[*nhx-2p::rde-1* + *rol-6(su1006)*], RNAi treatment is only effective in intestine⁸². In AMJ345 strain (jamSi2[*mex-5p::rde-1(+)*]II; *rde-1(ne219)V*), transgene rescues effective RNAi treatment in both intestine and germ line⁸³. TU3401 strain (*sid-1(pk3321)V*; uIs69[pCFJ90(*myo-2p::mCherry*) + *unc-119p::sid-1*]) was used for neuron-specific knockdown⁸⁴. All the aforementioned tissue-specific RNAi-sensitive strains were provided by the CGC. For tissue-specific RNAi experiments in the germ line alone, we used DCL569 strain (mksSi13[*sun-1p::rde-1::sun-1 3'UTR* + *unc-119(+)*]II; *rde-1(mkc36)V*)⁸⁵. DCL569 was a kind gift from Di Chen (Nanjing University, China).

For the generation of worm strains DVG146–DVG147 (N2, *ocbEx130[sur-5p::ZC373.1, myo-3p::GFP]* and N2, *ocbEx131[sur-5p::ZC373.1, myo-3p::GFP]*), a DNA plasmid mixture containing 70 ng μl^{-1} of the plasmid *sur5-p::cbs-1* and 20 ng μl^{-1} pPD93_97 (*myo3-p::GFP*) was injected into the gonads of adult N2 hermaphrodite animals, using standard methods⁸⁶. GFP-positive F₁ progeny were selected. Individual F₂ worms were isolated to establish independent lines. Following this method we also generated the worm strains DVG162 (N2, *ocbEx145[rgef-1p::ZC373.1, myo3-p::GFP]*), DVG163 (N2, *ocbEx146[rgef-1p::ZC373.1, myo3-p::GFP]*), DVG166 (N2, *ocbEx149[gly-19p::ZC373.1, myo-3p::GFP]*), DVG167 (N2, *ocbEx150[gly-19p::ZC373.1, myo-3p::GFP]*), DVG173 (N2, *ocbEx156[myo-3p::ZC373.1, myo-3p::GFP]*) and DVG174 (N2, *ocbEx157[myo-3p::ZC373.1, myo-3p::GFP]*). Control worms DVG9 (N2, *ocbEx9[myo3p::GFP]*) were generated by microinjecting N2 worms with 20 ng μl^{-1} pPD93_97²⁵. DVG186 (*glp-1(e2141)III*; *ocbEx150[gly-19p::ZC373.1, myo-3p::GFP]*) was generated by crossing DVG167 to CB4037.

For the generation of *cbs-1* transcriptional reporter line DVG156 (N2, *ocbEx140[ZC373.1p::GFP, pRF4(rol-6)]*), a DNA plasmid mixture containing 50 ng μl^{-1} of the plasmid pDV184 and 30 ng μl^{-1} pAD126 (pRF4(*rol-6*)) was injected into the gonads of adult N2 hermaphrodite animals. Roller-phenotype-positive F₁ progeny were selected. Individual F₂ worms were isolated to establish independent lines. Similarly, we generated the *cbs-1* transcriptional reporter line DVG185 by injecting a mixture of the plasmid pDV184 and pAD126 into the gonads of DCL569 germline-specific RNAi strain.

To generate DVG177 strain (*ocbEx160[cbs-1p::GFP, pRF4(rol-6)]*; *pges-2(ok3316)IV*), DVG156 was crossed to AA1724. Roller-phenotype-positive F₁ progeny were selected and transferred to individual plates. Screening of *pges-2(ok3316)* homozygote worms was done in F₂ progeny by PCR using the following primers: TGAACGCTGAGCATCCATAG and CGCCCGTTTTCTTTAATG.

RNAi constructs

RNAi-treated strains were fed *E. coli* (HT115) containing an empty control vector (L4440) or expressing double-stranded RNAi. *pgl-1*, *pgl-3*, *glh-1*, *mog-4*, *mog-5*, *iff-1*, *iff-2*, *ifg-1*,

ife-2, *rps-15*, *rsk-1*, *cct-2*, *cct-6*, *cct-8*, *hint-1*, *hsp-1*, *fk-6*, *ttr-6*, *cal-5* and *gld-1* RNAi constructs were obtained from the Vidal RNAi library. *glh-4*, *mog-1*, *eif-2A*, *cct-5*, *ama-1*, *cbs-1*, *nlp-24*, *daf-41* and *mrp-6* RNAi constructs were obtained from the Ahringer RNAi library. All constructs were sequence verified. For each RNAi, we assessed the knockdown efficiency at the distinct temperatures the RNAi was used (Supplementary Fig. 33).

Lifespan studies

In most of the lifespan experiments, synchronized larvae were raised and fed OP50 *E. coli* at 20 °C until day 1 of adulthood. If wild-type larvae were raised at 25 °C, this was noted in the figure (e.g., Fig. 1f-g and Fig. 3b). In experiments containing *glp-1*, *glp-4*, *fer-15;fem-1*, *fog-1*, *fog-2* or *spe-26* mutants, larvae were raised at the restrictive temperature (25 °C) to obtain germline-lacking and sterile worms. Once worms reached adulthood, they were shifted to a given temperature (i.e., 10 °C, 15 °C, 20 °C or 25 °C) on plates with HT115 *E. coli* carrying empty vector or RNAi clones. 96 animals were used per condition and scored every day or every other day²⁵. From the initial worm population, the worms that are lost or burrow into the medium as well as those that exhibit ‘protruding vulva’ or undergo bagging were censored. $n = \text{total number of uncensored animals} / \text{total number (uncensored+censored)}$ of animals observed in each experiment. Lifespans were conducted at the temperatures indicated in the corresponding figure. For non-integrated lines DVG9, DVG146, DVG147, DV162, DV163, DVG166, DVG167, DVG173 and DVG174, GFP-positive worms were selected for lifespan studies. PRISM 6 software was used to determine median lifespan and generate lifespan graphs. OASIS software was used for statistical analysis to determine mean lifespan⁸⁷. *P* values were calculated using the log-rank (Mantel–Cox) method. The *P* values refer to experimental and control animals in a single experiment. In the main text, each graph shows a representative experiment. See Supplementary Data 3 for statistical analysis and replicate data.

Construction of *cbs-1 C. elegans* expression plasmids

To construct the *C. elegans* plasmid (pDV163) for ubiquitous somatic overexpression of *cbs-1*, pPD95.77 from the Fire Lab kit was digested with SphI and XmaI to insert 3.6KB of the *sur-5* promoter. The resultant vector was then digested with KpnI and EcoRI to excise GFP and insert a multi-cloning site. ZC373.1a (*cbs-1*) was PCR amplified from cDNA to include 5′ NheI and 3′ NotI restriction sites and then cloned into the aforementioned vector. To generate neuronal-specific overexpression *cbs-1* plasmid (pDV188), pMS1 plasmid (*rgef-1p::rpn-6.1::unc-54 3′ UTR*) with an inserted multi-cloning site was digested with 5′ NheI and 3′ NotI restriction sites. Then, *cbs-1* was PCR amplified from cDNA to include 5′ NheI and 3′ NotI restriction sites and cloned into pMS1. Following the same strategy, *cbs-1* was cloned into pMS2 (*gly-19p::rpn-6.1::unc-54 3′ UTR*) to construct intestinal-specific expression plasmid (pDV189). To generate muscle-specific expression plasmid (pDV190), pMS3 plasmid (*myo-3p::rpn-6.1::unc-54 3′ UTR*) was digested with 5′ XbaI and 3′ AscI restriction sites. All constructs were sequence verified. pMS1-3 were a gift from A. Dillin.

Construction of *cbs-1* transcriptional reporter construct

To construct pDV184, pPD95.77 from the Fire Lab kit was digested with SalI and BamHI. The promoter region and part of exon 1 of ZC373.1a (*cbs-1*) was PCR amplified from N2

gDNA to include -1428 to 187 and then cloned into the aforementioned vector using the same enzymes.

***cbs-1* transcriptional reporter experiments and imaging**

DVG156 worms were grown at 20 °C until day 1 of adulthood and then transferred onto plates with *E. coli* (HT115) expressing empty vector or double-stranded RNAi. Worms were then cultured until day 7 at the indicated temperatures in the respective figure. For FUdR treatment experiments, day 1 adults were transferred onto plates with *E. coli* (HT115) expressing empty vector covered with 100 µg ml⁻¹ FUdR. Adult worms were then grown until day 5 at the indicated temperatures under FUdR treatment. In rescue experiments, worms were transferred at day 5 adulthood onto plates with PGE2 (Tocris, #363-24-6) spotted on top of the bacterial lawn. For imaging, adult worms were immobilized using 0.1% Azide in M9 buffer and covered with cover slip. Images of whole worms were acquired with Zeiss Axio Zoom.V16 fluorescence microscope. To quantify GFP fluorescence, worms were outlined and quantified using ImageJ software.

Body size imaging and quantification

Images of worms were acquired with Zeiss Axio Zoom.V16 microscope. To quantify body size, the whole worm was outlined and quantified using ImageJ software.

Bromodeoxyuridine (BrdU) proliferation assays

Worms were incubated with 33mM solution of BrdU (Sigma-Aldrich) in S medium for 2h at 20 °C. Worms were washed with EBT buffer (1X egg buffer, 0.2 % Tween 20, 20 mM Sodium Azide). Worms were then decapitated to extract germ line on a coverslip and covered with a poly-lysine-coated microscope slide. The coverslip was removed and the slide was fast frozen on dry ice. Then, the slide was fixed in methanol for 2 min at -20 °C and washed with PBST (1X PBS and 0.1% Tween 20). DNA was denatured in 2M HCl for 45 min at room temperature followed by washing with PBST. After blocking for 30 min in PBST 10% donkey serum, anti-BrdU antibody (Abcam, ab6326, RRID:AB_305426) was added (1:250) followed by overnight incubation in a humid chamber. Anti-Rat IgG secondary antibody (Life Technologies, A11081, RRID:AB_141738) was added (1:500) for 2 h at room temperature. Finally, slides were mounted with Precision coverslip (Roth) using DAPI fluoromount-G (Southern Biotech 0100-20).

Egg counting

Synchronized animals were raised and fed OP50 *E. coli* at 20 °C or 25 °C until late L4 stage. Number of eggs during the self-reproductive period was measured by singly plating late L4 worms and cultured them at the distinct temperatures indicated in the corresponding figures. Each adult worm was then transferred to a new plate every 24 h and the previous plate was kept at the respective temperature for another 24 h when the number of alive progeny, visible as L1 larvae was scored to assess percentage of viable eggs. This procedure was repeated until no alive progenies were counted.

For egg counting after the self-reproductive period, worms were grown at the distinct temperatures indicated in the corresponding figures for 8 days during adulthood. Then,

worms were singly plated and mated for 48 h at the indicated temperatures with young males which were raised at 20°C. After mating, females were transferred to a new plate every 24 h and the previous plate was kept at the respective temperature for another 24 h when the number of alive progeny was scored. This procedure was repeated until no alive progenies were counted.

H₂S detection

H₂S production capacity was measured following the lead sulfide method²⁷. First, worms were homogenated in lysis buffer (PBS supplemented with 10 mM L-cysteine and 1 mM pyridoxal 5'-phosphate hydrate (PLP)) using a Precellys 24 homogenizer (Bertin technologies). 300 µg of the lysate was transferred onto a well of a 96-well plate. Then, lead acetate paper was placed directly over the well for detection of H₂S at 37°C. H₂S production was detected by the black precipitate, lead sulfide, resulting from the specific reaction between H₂S and lead acetate.

Western blot

Worms were lysed in protein lysis buffer (50 mM Tris-HCl, pH 7.8, 150 mM NaCl, 0.25% sodium deoxycholate, 1 mM EDTA and protease inhibitor (Roche)) using a Precellys 24 homogenizer. Worm lysates were centrifuged at 10,000 rpm for 10 min at 4 °C and the supernatant was collected. Protein concentrations were determined with standard BCA protein assay (Thermoscientific). 30 µg of total protein was separated by SDS-PAGE, transferred to nitrocellulose membranes (Millipore) and subjected to immunoblotting. Western blot analysis was performed with anti-PGES2 antibody (Bioss, bs-2639R, 1:500; RRID:AB_10860215) and α-tubulin (Sigma, T6199, 1:5,000; RRID:AB_477583).

C. elegans germline and gut immunostaining

Worms were washed with EBT buffer (1X egg buffer, 0.2 % Tween 20, 20 mM Sodium Azid), decapitated to extract germ line and intestine on a coverslip and covered with a poly-lysine-treated microscope slide. The slide was fast frozen on dry ice, fixed in methanol for 2 min at -20 °C and washed with PBST (1X PBS and 0.1 % Tween 20). Immunostaining was processed by blocking with 10 % donkey serum in PBST for 30 min followed by overnight incubation with anti-PGES2 antibody (Bioss, bs-2639R, 1:100; RRID:AB_10860215) at room temperature. Alexa Fluor 488 goat anti-rabbit IgG (Life Technologies, A11008, RRID: AB_143165, 1:500) was added for 2 h. Slides were mounted with DAPI fluoromount-G (Southern Biotech 0100-20).

PGE2 measurements

We quantified PGE2 levels using a PGE2 ELISA Kit (amsbio, AMS.E-EL-0034), following manufacturer's instructions. *fer-15;fem-1* control sterile worms were lysed in protein lysis buffer (50 mM Tris-HCl, pH 7.8, 150 mM NaCl, 0.25% sodium deoxycholate, 1 mM EDTA and protease inhibitor (Roche)) using a Precellys 24 homogenizer. Worm lysates were centrifuged at 10,000 rpm for 10 min at 4°C and supernatant was collected. Protein concentrations were determined with standard BCA protein assay (Thermoscientific). 3 mg of total protein were used for measurement.

Oxygen consumption

Oxygen consumption rates were measured using an Oroboros Oxygraph 2k (Oroboros Instruments GmbH). 300 adult worms were used for each measurement. Data was analyzed using DatLab7 software (version 7 3.0.3).

Motility assay

At day 6 of adulthood, worms were transferred to a drop of M9 buffer and after 30 s of adaptation the number of body bends was counted for 30 s. A body bend is defined as change in direction of the bend at the mid-body.

Sample preparation for label-free quantitative proteomics and analysis

fer-15;fem-1 control sterile worms were lysed in urea buffer (8 M urea, 2 M Thiourea, 10 mM HEPES, pH 7.6) by sonication and cleared using centrifugation (13,000 rpm, 10 min). Supernatants were reduced (1 mM DTT, 30 min), alkylated (5 mM iodoacetamide (IAA), 45 min) and digested with trypsin at a 1:100 w/w ratio after diluting urea concentration to 2 M. One day after, samples were cleared (16,000g, 20 min) and supernatant was acidified. Peptides were cleaned up using stage tip extraction. The liquid chromatography tandem mass spectrometry (LC-MS/MS) equipment consisted out of an EASY nLC 1000 coupled to the quadrupole based QExactive instrument (Thermo Scientific) via a nano-spray electroionization source. Peptides were separated on an in-house packed 50 cm column (1.9 μ m C18 beads, Dr. Maisch) using a binary buffer system: A) 0.1% formic acid and B) 0.1% formic acid in acetonitrile. The content of buffer B was raised from 7% to 23% within 120 min and followed by an increase to 45% within 10 min. Then, within 5 min buffer B fraction was raised to 80% and held for further 5 min after which it was decreased to 5% within 2 min and held there for further 3 min before the next sample was loaded on the column. Eluting peptides were ionized by an applied voltage of 2.2 kV. The capillary temperature was 275°C and the S-lens RF level was set to 60. MS1 spectra were acquired using a resolution of 70,000 (at 200 m/z), an Automatic Gain Control (AGC) target of 3e6 and a maximum injection time of 20 ms in a scan range of 300-1750 Th. In a data dependent mode, the 10 most intense peaks were selected for isolation and fragmentation in the HCD cell using a normalized collision energy of 25 at an isolation window of 2.1 Th. Dynamic exclusion was enabled and set to 20 s. The MS/MS scan properties were: 17,500 resolution at 200 m/z, an AGC target of 5e5 and a maximum injection time of 60 ms. All label-free proteomics data sets were analyzed with the MaxQuant software (version 1.5.3.8). We employed the LFQ mode and used MaxQuant default settings for protein identification and LFQ quantification⁸⁸. All downstream analyses were carried out on LFQ values with Perseus (v. 1.5.2.4).

RNA isolation and sequencing

RNA from extruded germ lines of day 6-adult N2 worms was extracted using RNABee (Tel-Test Inc.). Libraries were prepared using the TruSeq Stranded mRNA Library Prep Kit. Library preparation started with 1 μ g total RNA. After selection (using poly-T oligo-attached magnetic beads), mRNA was purified and fragmented using divalent cations under elevated temperature. The RNA fragments underwent reverse transcription using random

primers followed by second strand cDNA synthesis with DNA Polymerase I and RNase H. After end repair and A-tailing, indexing adapters were ligated. The products were then purified and amplified (20 μ l template, 14 PCR cycles) to create the final cDNA libraries. After library validation and quantification (Agilent 2100 Bioanalyzer), equimolar amounts of library were pooled. The pool was quantified by using the Peqlab KAPA Library Quantification Kit and the Applied Biosystems 7900HT Sequence Detection System. The pool was sequenced on an Illumina HiSeq 4000 sequencer with a paired-end (2x75bp) protocol.

RNA-seq data were analysed using a QuickNGS pipeline⁸⁹. This workflow system provided basic read quality check using FastQC (version 0.10.1) and read statistics using SAMtools (version 0.1.19). The basic data processing of the QuickNGS pipeline consists of a splicing-aware alignment using Tophat2 (version 2.0.10) followed by reference-guided transcriptome reassembly with Cufflinks2 (version 2.1.1). The QuickNGS pipeline calculated read count means, fold change and *P*-values with DEseq2 (version 1.4.5) and gene expression for the individual samples with Cufflinks2 (version 2.1.1) as FPKMs, using in both cases genomic annotation from the Ensembl database version 87.

Quantitative RT-PCR

Total RNA was isolated from ~2,000 synchronized day 5-adult worms using RNAbee (Tel-Test Inc.). cDNA was generated using qScript Flex cDNA synthesis kit (Quantabio). SybrGreen real-time qPCR experiments were performed with a 1:20 dilution of cDNA using a CFC384 Real-Time System (Bio-Rad). Data were analysed with the comparative 2^{-C_t} method using the geometric mean of *cdc-42* and *pmp-3* as housekeeping genes⁹⁰. See Supplementary Table 2 for details about the primers used for this assay.

Supplementary Material

Refer to Web version on PubMed Central for supplementary material.

Acknowledgements

This work was supported by the European Research Council (ERC Starting Grant-677427 StemProteostasis) and the Deutsche Forschungsgemeinschaft (DFG) (VI742/1-2 and CECAD). We are grateful to E. Llamas for the graphical model and the germline scheme. We thank U. Pham and Niels Fritsma for their help in BrdU and lifespan experiments, respectively. We thank J.P. Derks for data analysis and preparation of heat map figures with R stats package of proteomics experiments. We also thank J. Horák for generation of tissue-specific *cbs-1* expression plasmids. We thank T. Hoppe for critical comments on the manuscript. We are grateful to the CECAD Proteomics and Imaging Facilities for their advice and contribution to proteomics and imaging experiments, respectively. We would also like to thank P. Wagle from the CECAD Bioinformatics Facility for data analysis of RNA-sequencing experiments.

Data availability

The authors declare that the main data supporting the findings of this study are available within the article and its supplementary files. Transcriptome data have been deposited in Gene Expression Omnibus (GEO) under the accession code GSE123054. All the other data are also available from the corresponding author upon request.

References

1. Fontana L, Partridge L, Longo VD. Extending healthy life span--from yeast to humans. *Science*. 2010; 328:321–326. [PubMed: 20395504]
2. Kenyon CJ. The genetics of ageing. *Nature*. 2010; 464:504–512. [PubMed: 20336132]
3. Robinson JD, Powell JR. Long-term recovery from acute cold shock in *Caenorhabditis elegans*. *BMC Cell Biol*. 2016; 17:2. [PubMed: 26754108]
4. Conti B. Considerations on temperature, longevity and aging. *Cell Mol Life Sci*. 2008; 65:1626–1630. [PubMed: 18425417]
5. Hosono R, Mitsui Y, Sato Y, Aizawa S, Miwa J. Life span of the wild and mutant nematode *Caenorhabditis elegans*. Effects of sex, sterilization, and temperature. *Exp Gerontol*. 1982; 17:163–172. [PubMed: 6213421]
6. Klass MR. Aging in the nematode *Caenorhabditis elegans*: major biological and environmental factors influencing life span. *Mech Ageing Dev*. 1977; 6:413–429. [PubMed: 926867]
7. Wu D, Rea SL, Cypser JR, Johnson TE. Mortality shifts in *Caenorhabditis elegans*: remembrance of conditions past. *Aging Cell*. 2009; 8:666–675. [PubMed: 19747231]
8. Lamb MJ. Temperature and lifespan in *Drosophila*. *Nature*. 1968; 220:808–809. [PubMed: 5698761]
9. Liu RK, Walford RL. Increased Growth and Life-Span with Lowered Ambient Temperature in Annual Fish *Cynolebias Adloffii*. *Nature*. 1966; 212:1277.
10. Valenzano DR, Terzibasi E, Cattaneo A, Domenici L, Cellierino A. Temperature affects longevity and age-related locomotor and cognitive decay in the short-lived fish *Nothobranchius furzeri*. *Aging Cell*. 2006; 5:275–278. [PubMed: 16842500]
11. Lee SJ, Kenyon C. Regulation of the longevity response to temperature by thermosensory neurons in *Caenorhabditis elegans*. *Curr Biol*. 2009; 19:715–722. [PubMed: 19375320]
12. Xiao R, et al. A genetic program promotes *C. elegans* longevity at cold temperatures via a thermosensitive TRP channel. *Cell*. 2013; 152:806–817. [PubMed: 23415228]
13. Conti B, et al. Transgenic mice with a reduced core body temperature have an increased life span. *Science*. 2006; 314:825–828. [PubMed: 17082459]
14. Loeb J, Northrop JH. Is There a Temperature Coefficient for the Duration of Life? *Proc Natl Acad Sci U S A*. 1916; 2:456–457. [PubMed: 16586628]
15. Zhang B, et al. Environmental Temperature Differentially Modulates *C. elegans* Longevity through a Thermosensitive TRP Channel. *Cell Rep*. 2015; 11:1414–1424. [PubMed: 26027928]
16. Zhang B, et al. Brain-gut communications via distinct neuroendocrine signals bidirectionally regulate longevity in *C. elegans*. *Genes Dev*. 2018; 32:258–270. [PubMed: 29491136]
17. Horikawa M, Sural S, Hsu AL, Antebi A. Co-chaperone p23 regulates *C. elegans* Lifespan in Response to Temperature. *PLoS Genet*. 2015; 11:e1005023. [PubMed: 25830239]
18. Partridge L, Gems D, Withers DJ. Sex and death: what is the connection? *Cell*. 2005; 120:461–472. [PubMed: 15734679]
19. Kirkwood TB. Evolution of ageing. *Nature*. 1977; 270:301–304. [PubMed: 593350]
20. Arantes-Oliveira N, Apfeld J, Dillin A, Kenyon C. Regulation of life-span by germ-line stem cells in *Caenorhabditis elegans*. *Science*. 2002; 295:502–505. [PubMed: 11799246]
21. Hsin H, Kenyon C. Signals from the reproductive system regulate the lifespan of *C. elegans*. *Nature*. 1999; 399:362–366. [PubMed: 10360574]
22. Vilchez D, et al. RPN-6 determines *C. elegans* longevity under proteotoxic stress conditions. *Nature*. 2012; 489:263–268. [PubMed: 22922647]
23. Berman JR, Kenyon C. Germ-cell loss extends *C. elegans* life span through regulation of DAF-16 by kri-1 and lipophilic-hormone signaling. *Cell*. 2006; 124:1055–1068. [PubMed: 16530050]
24. Lapierre LR, Gelino S, Melendez A, Hansen M. Autophagy and lipid metabolism coordinately modulate life span in germline-less *C. elegans*. *Curr Biol*. 2011; 21:1507–1514. [PubMed: 21906946]
25. Noormohammadi A, et al. Somatic increase of CCT8 mimics proteostasis of human pluripotent stem cells and extends *C. elegans* lifespan. *Nat Commun*. 2016; 7:13649. [PubMed: 27892468]

26. Shemesh N, Shai N, Ben-Zvi A. Germline stem cell arrest inhibits the collapse of somatic proteostasis early in *Caenorhabditis elegans* adulthood. *Aging Cell*. 2013
27. Hine C, et al. Endogenous hydrogen sulfide production is essential for dietary restriction benefits. *Cell*. 2015; 160:132–144. [PubMed: 25542313]
28. Miller DL, Roth MB. Hydrogen sulfide increases thermotolerance and lifespan in *Caenorhabditis elegans*. *Proc Natl Acad Sci U S A*. 2007; 104:20618–20622. [PubMed: 18077331]
29. Priess JR, Schnabel H, Schnabel R. The *glp-1* locus and cellular interactions in early *C. elegans* embryos. *Cell*. 1987; 51:601–611. [PubMed: 3677169]
30. Curran SP, Wu X, Riedel CG, Ruvkun G. A soma-to-germline transformation in long-lived *Caenorhabditis elegans* mutants. *Nature*. 2009; 459:1079–1084. [PubMed: 19506556]
31. Syntichaki P, Troulinaki K, Tavernarakis N. eIF4E function in somatic cells modulates ageing in *Caenorhabditis elegans*. *Nature*. 2007; 445:922–926. [PubMed: 17277769]
32. Andux S, Ellis RE. Apoptosis maintains oocyte quality in aging *Caenorhabditis elegans* females. *PLoS Genet*. 2008; 4:e1000295. [PubMed: 19057674]
33. Barton MK, Kimble J. *fog-1*, a regulatory gene required for specification of spermatogenesis in the germ line of *Caenorhabditis elegans*. *Genetics*. 1990; 125:29–39. [PubMed: 2341035]
34. L'Hernault SW. Spermatogenesis. *WormBook*. 2006:1–14.
35. Schedl T, Kimble J. *fog-2*, a germ-line-specific sex determination gene required for hermaphrodite spermatogenesis in *Caenorhabditis elegans*. *Genetics*. 1988; 119:43–61. [PubMed: 3396865]
36. Varkey JP, Muhlrud PJ, Minniti AN, Do B, Ward S. The *Caenorhabditis elegans* *spe-26* gene is necessary to form spermatids and encodes a protein similar to the actin-associated proteins *kelch* and *scruin*. *Genes Dev*. 1995; 9:1074–1086. [PubMed: 7744249]
37. Hubbard EJ, Greenstein D. Introduction to the germ line. *WormBook*. 2005:1–4.
38. Crittenden SL, Leonhard KA, Byrd DT, Kimble J. Cellular analyses of the mitotic region in the *Caenorhabditis elegans* adult germ line. *Mol Biol Cell*. 2006; 17:3051–3061. [PubMed: 16672375]
39. Kimble J, Seidel H. *StemBook*. 2008
40. Morita Y, Tilly JL. Oocyte apoptosis: like sand through an hourglass. *Dev Biol*. 1999; 213:1–17. [PubMed: 10452843]
41. Hodgkin J, Barnes TM. More is not better: brood size and population growth in a self-fertilizing nematode. *Proc Biol Sci*. 1991; 246:19–24. [PubMed: 1684664]
42. Garrity PA, Goodman MB, Samuel AD, Sengupta P. Running hot and cold: behavioral strategies, neural circuits, and the molecular machinery for thermotaxis in *C. elegans* and *Drosophila*. *Genes Dev*. 2010; 24:2365–2382. [PubMed: 21041406]
43. Glauser DA, et al. Heat Avoidance Is Regulated by Transient Receptor Potential (TRP) Channels and a Neuropeptide Signaling Pathway in *Caenorhabditis elegans*. *Genetics*. 2011; 188:91–U150. [PubMed: 21368276]
44. Kindt KS, et al. *Caenorhabditis elegans* TRPA-1 functions in mechanosensation. *Nat Neurosci*. 2007; 10:568–577. [PubMed: 17450139]
45. Perkins LA, Hedgecock EM, Thomson JN, Culotti JG. Mutant sensory cilia in the nematode *Caenorhabditis elegans*. *Dev Biol*. 1986; 117:456–487. [PubMed: 2428682]
46. Satterlee JS, et al. Specification of thermosensory neuron fate in *C. elegans* requires *txx-1*, a homolog of *otd/Otx*. *Neuron*. 2001; 31:943–956. [PubMed: 11580895]
47. Joshi PM, Riddle MR, Djabrayan NJ, Rothman JH. *Caenorhabditis elegans* as a model for stem cell biology. *Dev Dyn*. 2010; 239:1539–1554. [PubMed: 20419785]
48. Graham PL, Schedl T, Kimble J. More *mog* genes that influence the switch from spermatogenesis to oogenesis in the hermaphrodite germ line of *Caenorhabditis elegans*. *Dev Genet*. 1993; 14:471–484. [PubMed: 8111975]
49. Puoti A, Kimble J. The *Caenorhabditis elegans* sex determination gene *mog-1* encodes a member of the DEAH-Box protein family. *Mol Cell Biol*. 1999; 19:2189–2197. [PubMed: 10022905]
50. Puoti A, Kimble J. The hermaphrodite sperm/oocyte switch requires the *Caenorhabditis elegans* homologs of PRP2 and PRP22. *Proc Natl Acad Sci U S A*. 2000; 97:3276–3281. [PubMed: 10737793]

51. Kawasaki I, et al. The PGL family proteins associate with germ granules and function redundantly in *Caenorhabditis elegans* germline development. *Genetics*. 2004; 167:645–661. [PubMed: 15238518]
52. Kawasaki I, et al. PGL-1, a predicted RNA-binding component of germ granules, is essential for fertility in *C. elegans*. *Cell*. 1998; 94:635–645. [PubMed: 9741628]
53. Kuznicki KA, et al. Combinatorial RNA interference indicates GLH-4 can compensate for GLH-1; these two P granule components are critical for fertility in *C. elegans*. *Development*. 2000; 127:2907–2916. [PubMed: 10851135]
54. Hanazawa M, et al. The *Caenorhabditis elegans* eukaryotic initiation factor 5A homologue, IFF-1, is required for germ cell proliferation, gametogenesis and localization of the P-granule component PGL-1. *Mech Dev*. 2004; 121:213–224. [PubMed: 15003625]
55. Green RA, et al. A high-resolution *C. elegans* essential gene network based on phenotypic profiling of a complex tissue. *Cell*. 2011; 145:470–482. [PubMed: 21529718]
56. Francis R, Barton MK, Kimble J, Schedl T. *gld-1*, a tumor suppressor gene required for oocyte development in *Caenorhabditis elegans*. *Genetics*. 1995; 139:579–606. [PubMed: 7713419]
57. Marin VA, Evans TC. Translational repression of a *C. elegans* Notch mRNA by the STAR/KH domain protein GLD-1. *Development*. 2003; 130:2623–2632. [PubMed: 12736207]
58. Pinkston JM, Garigan D, Hansen M, Kenyon C. Mutations that increase the life span of *C. elegans* inhibit tumor growth. *Science*. 2006; 313:971–975. [PubMed: 16917064]
59. Van Voorhies WA, Ward S. Genetic and environmental conditions that increase longevity in *Caenorhabditis elegans* decrease metabolic rate. *P Natl Acad Sci USA*. 1999; 96:11399–11403.
60. Vozdek R, Hnizda A, Krijt J, Kostrouchova M, Kozich V. Novel structural arrangement of nematode cystathionine beta-synthases: characterization of *Caenorhabditis elegans* CBS-1. *Biochem J*. 2012; 443:535–547. [PubMed: 22240119]
61. Yang G, et al. H₂S as a physiologic vasorelaxant: hypertension in mice with deletion of cystathionine gamma-lyase. *Science*. 2008; 322:587–590. [PubMed: 18948540]
62. Paul BD, Snyder SH. H₂S signalling through protein sulfhydration and beyond. *Nat Rev Mol Cell Bio*. 2012; 13:499–507. [PubMed: 22781905]
63. Kudo I, Murakami M. Prostaglandin E synthase, a terminal enzyme for prostaglandin E₂ biosynthesis. *J Biochem Mol Biol*. 2005; 38:633–638. [PubMed: 16336776]
64. Tanioka T, et al. Regulation of cytosolic prostaglandin E₂ synthase by 90-kDa heat shock protein. *Biochem Biophys Res Commun*. 2003; 303:1018–1023. [PubMed: 12684036]
65. Lovgren AK, Kovarova M, Koller BH. cPGES/p23 is required for glucocorticoid receptor function and embryonic growth but not prostaglandin E-2 synthesis. *Molecular and Cellular Biology*. 2007; 27:4416–4430. [PubMed: 17438133]
66. Kochel TJ, Fulton AM. Multiple drug resistance-associated protein 4 (MRP4), prostaglandin transporter (PGT), and 15-hydroxyprostaglandin dehydrogenase (15-PGDH) as determinants of PGE₂ levels in cancer. *Prostaglandins Other Lipid Mediat*. 2015; 116–117:99–103.
67. Taylor RC, Berendzen KM, Dillin A. Systemic stress signalling: understanding the cell non-autonomous control of proteostasis. *Nat Rev Mol Cell Biol*. 2014; 15:211–217. [PubMed: 24556842]
68. Khodakarami A, Mels J, Saez I, Vilchez D. Mediation of organismal aging and somatic proteostasis by the germline. *Frontiers in Molecular Biosciences*. 2015; 2
69. Prahlad V, Cornelius T, Morimoto RI. Regulation of the cellular heat shock response in *Caenorhabditis elegans* by thermosensory neurons. *Science*. 2008; 320:811–814. [PubMed: 18467592]
70. Gandhi S, Santelli J, Mitchell DH, Stiles JW, Raosanadi D. A Simple Method for Maintaining Large, Aging Populations of *Caenorhabditis-Elegans*. *Mechanisms of Ageing and Development*. 1980; 12:137–150. [PubMed: 6445025]
71. Mitchell DH, Stiles JW, Santelli J, Rao SD. Synchronous Growth and Aging of *Caenorhabditis-Elegans* in the Presence of Fluorodeoxyuridine. *J Gerontol*. 1979; 34:28–36. [PubMed: 153363]
72. Van Raamsdonk JM, Hekimi S. FUDR causes a twofold increase in the lifespan of the mitochondrial mutant *gas-1*. *Mech Ageing Dev*. 2011; 132:519–521. [PubMed: 21893079]

73. Feldman N, Kosolapov L, Ben-Zvi A. Fluorodeoxyuridine improves *Caenorhabditis elegans* proteostasis independent of reproduction onset. *PLoS One*. 2014; 9:e85964. [PubMed: 24465816]
74. Scott TA, et al. Host-Microbe Co-metabolism Dictates Cancer Drug Efficacy in *C. elegans*. *Cell*. 2017; 169:442–456 e418. [PubMed: 28431245]
75. Wei Y, Kenyon C. Roles for ROS and hydrogen sulfide in the longevity response to germline loss in *Caenorhabditis elegans*. *Proc Natl Acad Sci U S A*. 2016; 113:E2832–2841. [PubMed: 27140632]
76. O'Rourke EJ, Kuballa P, Xavier R, Ruvkun G. omega-6 Polyunsaturated fatty acids extend life span through the activation of autophagy. *Gene Dev*. 2013; 27:429–440. [PubMed: 23392608]
77. Gold EB. The timing of the age at which natural menopause occurs. *Obstet Gynecol Clin North Am*. 2011; 38:425–440. [PubMed: 21961711]
78. Ossewaarde ME, et al. Age at menopause, cause-specific mortality and total life expectancy. *Epidemiology*. 2005; 16:556–562. [PubMed: 15951675]
79. Shadyab AH, et al. Ages at menarche and menopause and reproductive lifespan as predictors of exceptional longevity in women: the Women's Health Initiative. *Menopause*. 2017; 24:35–44. [PubMed: 27465713]
80. Brenner S. The genetics of *Caenorhabditis elegans*. *Genetics*. 1974; 77:71–94. [PubMed: 4366476]
81. Yigit E, et al. Analysis of the *C. elegans* Argonaute family reveals that distinct Argonautes act sequentially during RNAi. *Cell*. 2006; 127:747–757. [PubMed: 17110334]
82. Espelt MV, Estevez AY, Yin X, Strange K. Oscillatory Ca²⁺ signaling in the isolated *Caenorhabditis elegans* intestine: role of the inositol-1,4,5-trisphosphate receptor and phospholipases C beta and gamma. *J Gen Physiol*. 2005; 126:379–392. [PubMed: 16186564]
83. Marre J, Traver EC, Jose AM. Extracellular RNA is transported from one generation to the next in *Caenorhabditis elegans*. *Proc Natl Acad Sci U S A*. 2016; 113:12496–12501. [PubMed: 27791108]
84. Calixto A, Chelur D, Topalidou I, Chen X, Chalfie M. Enhanced neuronal RNAi in *C. elegans* using SID-1. *Nat Methods*. 2010; 7:554–559. [PubMed: 20512143]
85. Zou L, et al. Construction of a germline-specific RNAi tool in *C. elegans*. *Sci Rep*. 2019; 9:2354. [PubMed: 30787374]
86. Mello CC, Kramer JM, Stinchcomb D, Ambros V. Efficient gene transfer in *C. elegans*: extrachromosomal maintenance and integration of transforming sequences. *EMBO J*. 1991; 10:3959–3970. [PubMed: 1935914]
87. Yang JS, et al. OASIS: online application for the survival analysis of lifespan assays performed in aging research. *PLoS One*. 2011; 6:e23525. [PubMed: 21858155]
88. Cox J, et al. Accurate proteome-wide label-free quantification by delayed normalization and maximal peptide ratio extraction, termed MaxLFQ. *Mol Cell Proteomics*. 2014; 13:2513–2526. [PubMed: 24942700]
89. Wagle P, Nikolic M, Frommolt P. QuickNGS elevates Next-Generation Sequencing data analysis to a new level of automation. *BMC Genomics*. 2015; 16:487. [PubMed: 26126663]
90. Hoogewijs D, Houthoofd K, Matthijssens F, Vandesompele J, Vanfleteren JR. Selection and validation of a set of reliable reference genes for quantitative sod gene expression analysis in *C. elegans*. *BMC Mol Biol*. 2008; 9:9. [PubMed: 18211699]

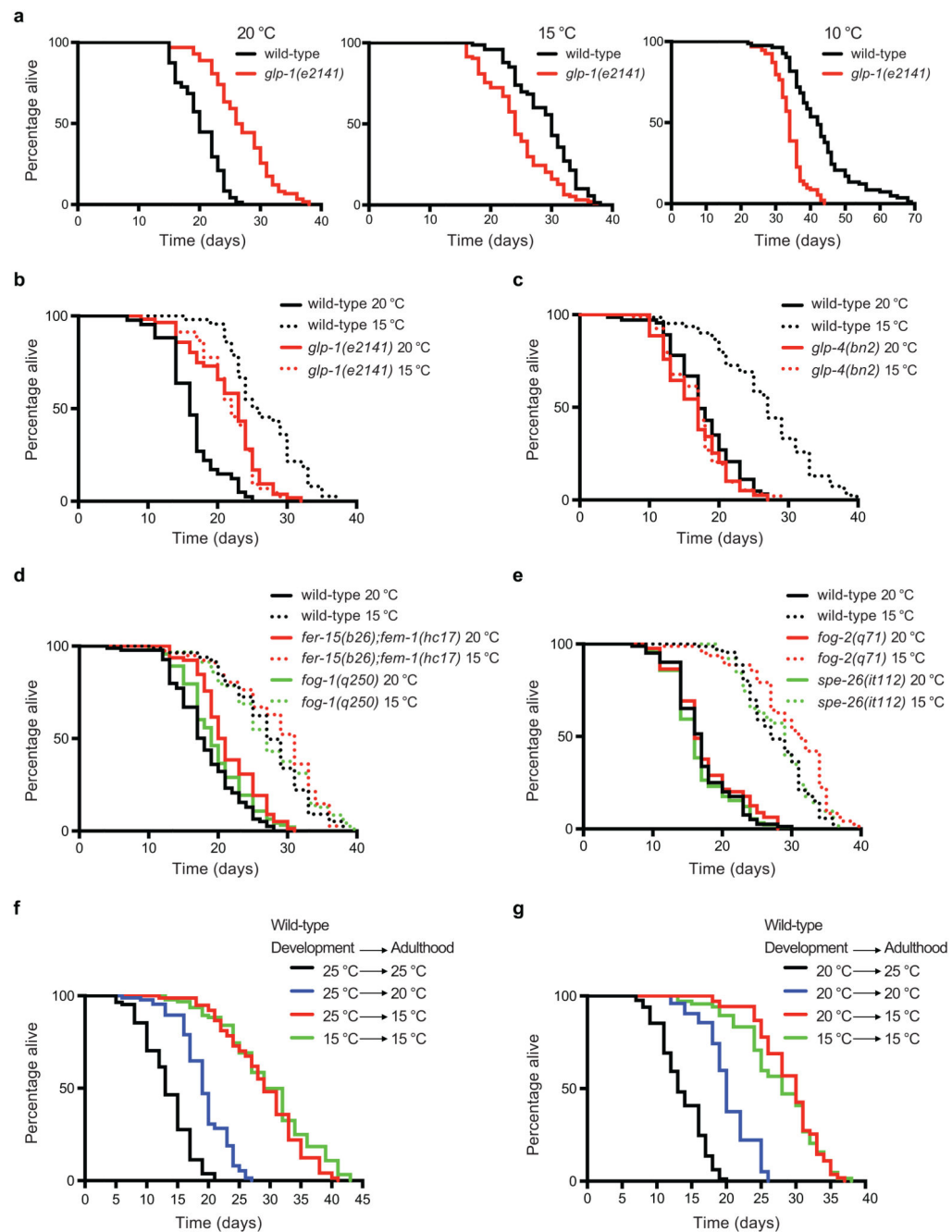


Figure 1. The germ line is essential for cold-induced longevity during adulthood.

a, Germline-lacking worms (*glp-1(e2141)*) are long lived compared to wild-type (N2) strain at 20°C (N2 20°C mean \pm s.e.m: 20.15 \pm 0.40, *glp-1* 20°C: 26.90 \pm 0.58, $P < 0.0001$). In contrast, germline-lacking worms are short lived in comparison with wild-type worms at cold temperatures (N2 15°C: 29.01 \pm 0.58, *glp-1* 15°C: 24.39 \pm 0.56, $P < 0.0001$; N2 10°C: 42.94 \pm 1.05, *glp-1* 10°C: 33.95 \pm 0.46, $P < 0.0001$). **b**, Temperature reduction (15°C) extends lifespan of wild-type worms (N2 20°C mean \pm s.e.m: 16.40 \pm 0.60, N2 15°C: 26.73 \pm 0.77, $P < 0.0001$) but not *glp-1* germline-lacking worms (*glp-1* 20°C: 21.59 \pm 0.66, *glp-1* 15°C:

21.78 ± 0.60, P= 0.6396). Wild-type worms are long lived compared with *glp-1* mutant worms at cold temperature (*N2* 15°C versus *glp-1* 15°C, P<0.0001). **c**, Temperature reduction extends lifespan of wild-type worms (*N2* 20°C mean ± s.e.m: 17.83 ± 0.58, *N2* 15°C: 26.81 ± 0.90, P<0.0001) but not *glp-4(bn2)* germline-lacking worms (*glp-4* 20°C: 16.44 ± 0.49, *glp-4* 15°C: 16.71 ± 0.45, P= 0.7379). Wild-type worms are long lived compared with *glp-4* mutant worms at cold temperature (*N2* 15°C versus *glp-4* 15°C, P<0.0001). **d**, Temperature reduction extends lifespan of sterile *fer-15(b26);fem-1(hc17)* and *fog-1(q250)* mutant worms with a proliferating germ line. *N2* 20°C mean ± s.e.m: 18.17 ± 0.53 versus *N2* 15°C: 27.20 ± 0.67, P<0.0001; *fer-15;fem-1* 20°C: 21.42 ± 0.50 versus *fer-15;fem-1* 15°C: 28.46 ± 0.74, P<0.0001; *fog-1* 20°C: 19.62 ± 0.49 versus *fog-1* 15°C: 27.22 ± 0.70, P<0.0001. **e**, Temperature reduction (15°C) extends lifespan of sterile *fog-2(q71)* and *spe-26(it112)* mutant worms with a proliferating germ line. *N2* 20°C mean ± s.e.m: 17.01 ± 0.48 versus *N2* 15°C: 27.79 ± 0.60, P<0.0001; *fog-2* 20°C: 16.55 ± 0.46 versus *fog-2* 15°C: 27.94 ± 0.62, P<0.0001; *spe-26* 20°C: 17.51 ± 0.54 versus *spe-26* 15°C: 29.96 ± 0.67, P<0.0001. **f**, Wild-type larvae were raised at 25°C and then adult worms were shifted to the indicated temperatures. Exposure to low temperature (15°C) during adulthood is sufficient to extend longevity (P<0.0001). 25°C (development and adulthood) mean ± s.e.m: 13.38 ± 0.43, shifted to 20°C after development: 19.28 ± 0.44, shifted to 15°C after development: 29.07 ± 0.72, 15°C (development and adulthood): 29.89 ± 0.76. **g**, After development at 20°C, adult wild-type worms were shifted to the indicated temperatures. Exposure to low temperature during adulthood extends longevity (P<0.0001). 20°C (development and adulthood) mean ± s.e.m: 20.25 ± 0.44, shifted to 25°C after development: 13.66 ± 0.37, shifted to 15°C after development: 29.11 ± 0.53, 15°C (development and adulthood): 26.65 ± 0.70. P-values: two-sided log-rank test, n= 96 worms/condition. See Supplementary Data 3 for statistical analysis and replicate data of lifespan experiments.

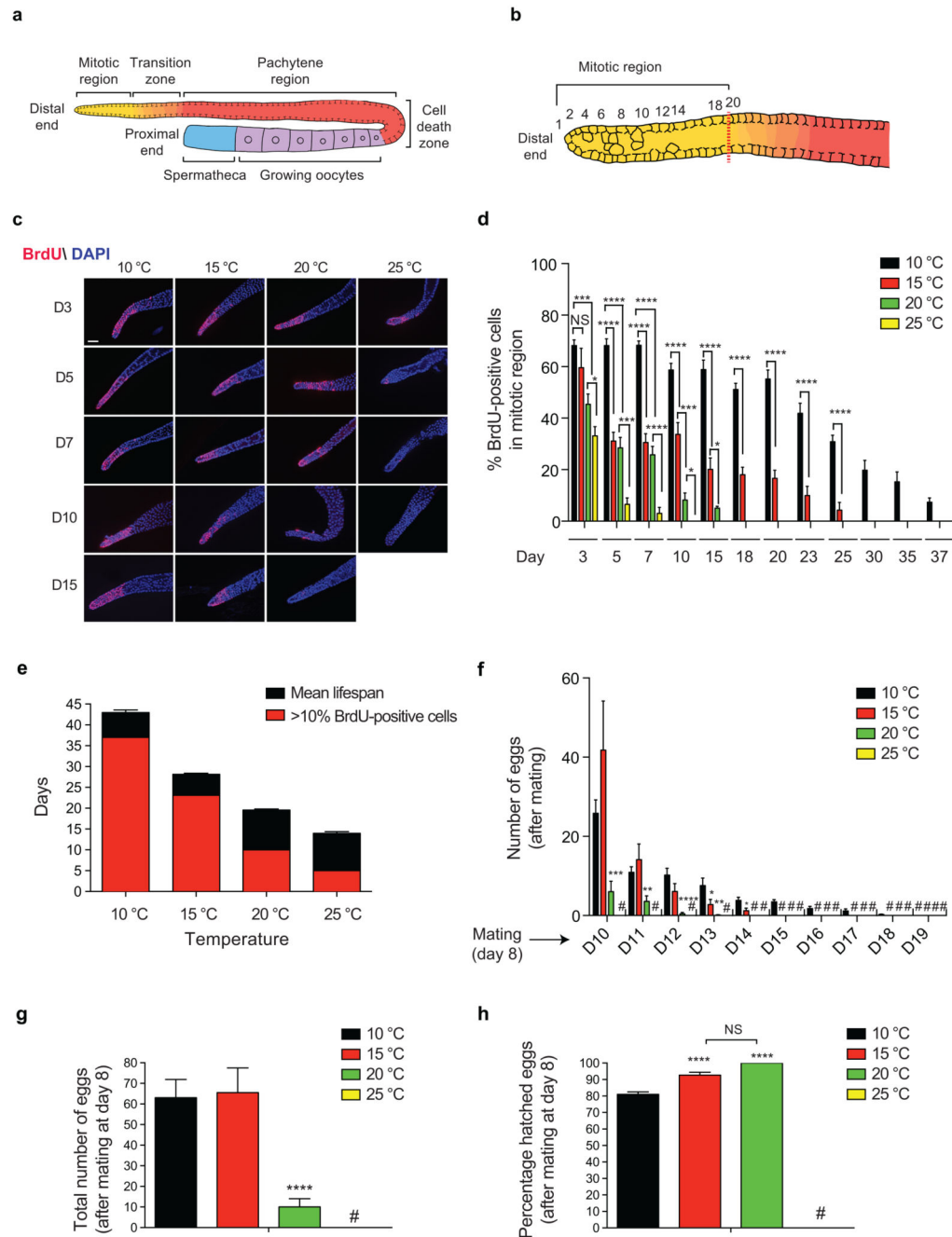


Figure 2. Cold temperature delays exhaustion of GSCs and reproductive aging.

a, Schematic representation of one gonad of the young adult hermaphrodite germ line. Germ cells are derived from proliferating GSCs located at the mitotic region. Proliferating cells enter meiosis and move proximally from the mitotic region to the meiotic zones (transition zone, pachytene). Germ cell apoptosis occurs in the germline loop region (death cell zone). GSCs generate sperm during larval stages, then switch to oocyte production during adulthood. **b**, Representation of the mitotic region. Red dashed line corresponds to the point at which multiple germ cells exhibit an early meiotic phenotype, considered the boundary

between the mitotic region and the transition zone (row 20 of cells from the most distal cell). **c**, Bromodeoxyuridine (BrdU) staining of proliferating germ cells. Wild-type *C. elegans* were shifted to the distinct temperatures during adulthood and the germ lines were extruded after 2 h BrdU treatment at the indicated day (D) of age. Cell nuclei were stained with DAPI. Scale bar represents 20 μm . The images are representative of 4 independent experiments. **d**, Graph represents the percentage of BrdU-positive cells/total nuclei within the mitotic region (mean \pm s.e.m., 10°C D3-37, 15°C D3-23 (n=20 germ lines), 15°C D23, 20°C D3-15, 25°C D3-10 (n= 15), germ lines were scored from 3 independent experiments). We did not examine the germ line after D15 at 25°C, D18 at 20°C, D25 at 15°C and D37 at 10°C as the percentage of BrdU-positive cells was below 10% at these ages/temperatures. NS= not significant (P=0.3322). **e**, Graph represents the average \pm s.e.m. of the mean lifespan at 10°C (n= 15 independent experiments), 15°C (n= 56), 20°C (n= 29) and 25°C (n= 22). The graph also indicates until what day of the respective mean lifespan is germ cell proliferation maintained at each temperature (>10% BrdU-positive cells in the mitotic region), as inferred from the data presented in the previous panel. **f**, Adult worms were cultured at the indicated temperature during adulthood. After the self-reproductive period, worms were mated at day 8 of adulthood with young males raised at 20°C and kept at the respective temperatures. Graph represents the number of eggs laid per worm every 24 h after mating (mean \pm s.e.m., n= 24 worms scored per condition from 3 independent experiments). (#) no eggs were laid. **g**, Total number of eggs laid per worm at different temperatures after mating at day 8 of adulthood (mean \pm s.e.m., n= 24 worms from 3 independent experiments). (#) no eggs were laid by mated worms at 25°C. **h**, Percentage of hatched eggs at different temperatures (mean \pm s.e.m., n= 24 worms from 3 independent experiments). The percentage of viable eggs after mating is similar at 15°C and 20°C (NS= not significant, P=0.0715). Although egg hatching decreases at 10°C, most of the eggs (81%) were still viable. (#) no eggs were laid. Statistical comparisons were made by two-tailed Student's t-test for unpaired samples. P-value: *(P<0.05), **(P<0.01), ***(P<0.001), ****(P<0.0001).

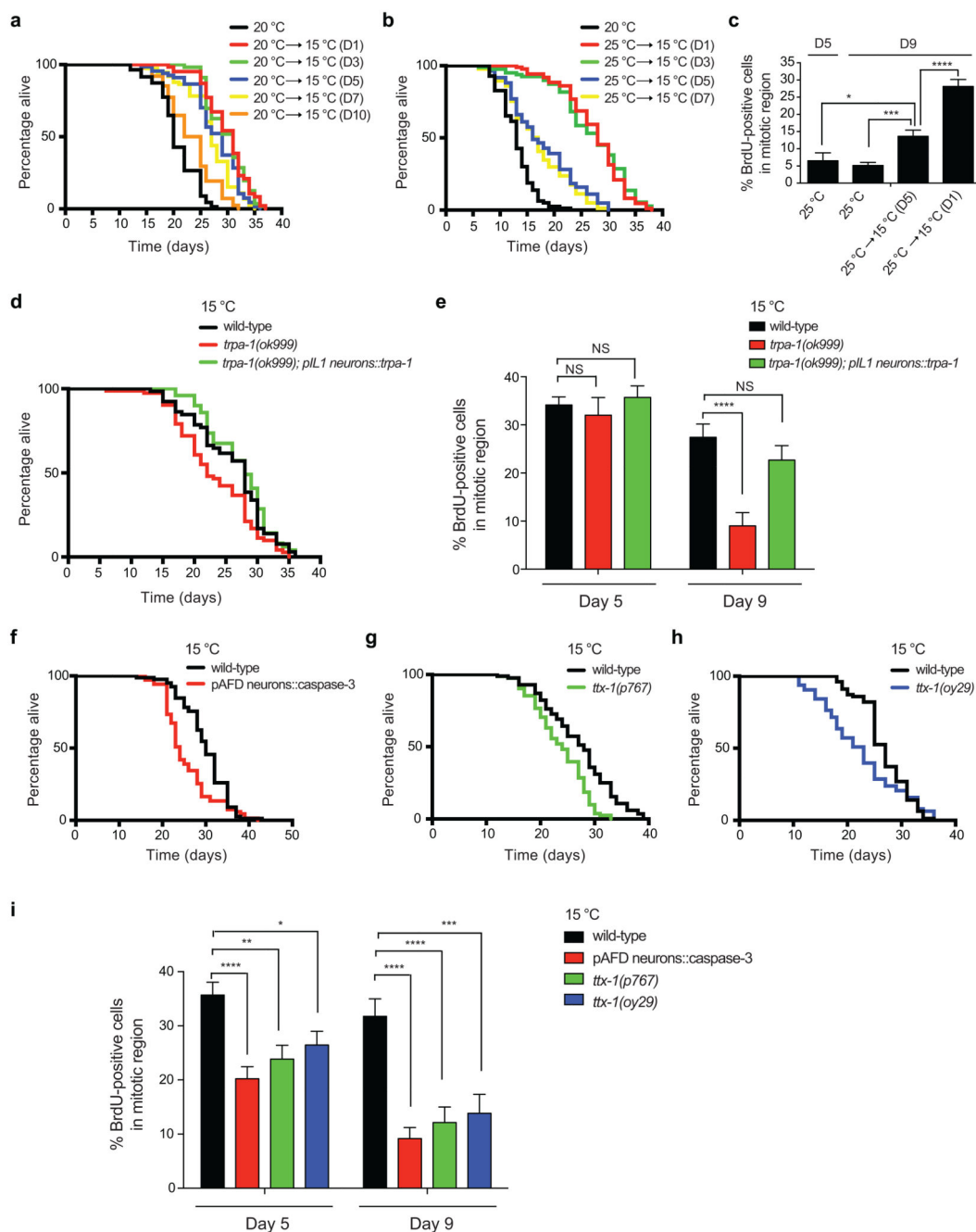


Figure 3. Thermosensory neurons regulate cold-induced longevity and GSC proliferation.

a, Lifespan of worms at 20°C shifted to lower temperature (15°C) at the indicated days (D). 20°C mean \pm s.e.m: 20.72 ± 0.43 , shifted to 15°C at D1: 29.85 ± 0.52 ($P < 0.0001$), shifted to 15°C at D3: 29.86 ± 0.49 ($P < 0.0001$), shifted to 15°C at D5: 27.75 ± 0.58 ($P < 0.0001$), shifted to 15°C at D7: 26.92 ± 0.53 ($P < 0.0001$), shifted to 15°C at D10: 23.26 ± 0.48 ($P < 0.0001$). Cold-induced longevity decreases when worms are shifted to lower temperature at day 10 (D10 versus D1-7, $P < 0.0001$). **b**, Lifespan of worms at 25°C shifted to 15°C at different days. 25°C mean \pm s.e.m: 13.09 ± 0.35 , shifted to 15°C at D1: 27.43 ± 0.60

($P < 0.0001$), shifted to 15°C at D3: 26.90 ± 0.80 ($P < 0.0001$), shifted to 15°C at D5: 17.74 ± 0.68 ($P < 0.0001$), shifted to 15°C at D7: 16.98 ± 0.62 ($P < 0.0001$). Cold-induced longevity decreases when worms are shifted to lower temperature at day 5 (D5 versus D1-3, $P < 0.0001$). Worms shifted to 15°C at either day 5 or day 7 exhibit a similar lifespan ($P < 0.2661$). **c**, Percentage of BrdU-positive cells/total nuclei within the mitotic region (mean \pm s.e.m., 25°C D5 and D9 (n=16 germ lines), shifted to 15°C at D1 or D5 (n=20), germ lines from 2 independent experiments). Worms were maintained at 25°C until BrdU analysis (D5 and D9) or shifted to 15°C at the indicated days before BrdU analysis at D9 of adulthood. NS= not significant (D5: WT versus *trpa-1* ($P = 0.6091$); WT vs *trpa-1;pIL1::trpa-1* ($P = 0.5948$). D9: WT vs *trpa-1;pIL1::trpa-1* ($P = 0.2502$). **d**, Transgenic expression of *trpa-1* in IL1 neurons driven by *aqp-6* promoter rescues the short-lived phenotype of *trpa-1* mutants at 15°C. Wild-type mean \pm s.e.m: 25.97 ± 0.73 , *trpa-1(ok999)*: 23.34 ± 0.72 ($P = 0.0127$), *trpa-1(ok999);pIL1::trpa-1*: 27.70 ± 0.70 ($P = 0.4163$). **e**, Expression of *trpa-1* in IL1 neurons rescues low germline proliferation in *trpa-1* mutant worms at 15°C. Graph represents the percentage of BrdU-positive cells/total nuclei in the indicated strains at day 5 and 9 of adulthood (mean \pm s.e.m., 15 germ lines from 2 independent experiments). **f**, Specific AFD ablation by driving reconstituted caspase-3 under *gcy-8* promoter reduces cold-induced longevity at 15°C (*N2* wild-type mean \pm s.e.m: 29.88 ± 0.58 , *pAFD::caspase-3*: 25.61 ± 0.69 , $P = 0.0002$). **g**, *ttx-1(p767)* mutant worms are short-lived at 15°C (*N2* mean \pm s.e.m: 27.05 ± 0.69 , *ttx-1(p767)*: 23.64 ± 0.54 , $P < 0.0001$). **h**, *ttx-1(oy29)* mutant worms are short-lived at 15°C (*N2* mean \pm s.e.m: 26.81 ± 0.50 , *ttx-1(oy29)*: 22.49 ± 0.91 , $P = 0.0267$). **i**, Percentage of BrdU-positive cells/total nuclei in the indicated strains at day 5 and 9 of adulthood (mean \pm s.e.m., D5 (n=30 germ lines), D9 (n=15), germ lines from 3 independent experiments). In lifespan experiments, P-values: two-sided log-rank test, n= 96 worms/condition (see Supplementary Data 3 for statistical analysis and replicate data). In Figures **3c**, **3e** and **3i**, statistical comparisons were made by two-tailed Student's t-test for unpaired samples. P-value: *($P < 0.05$), **($P < 0.01$), ***($P < 0.001$), ****($P < 0.0001$).

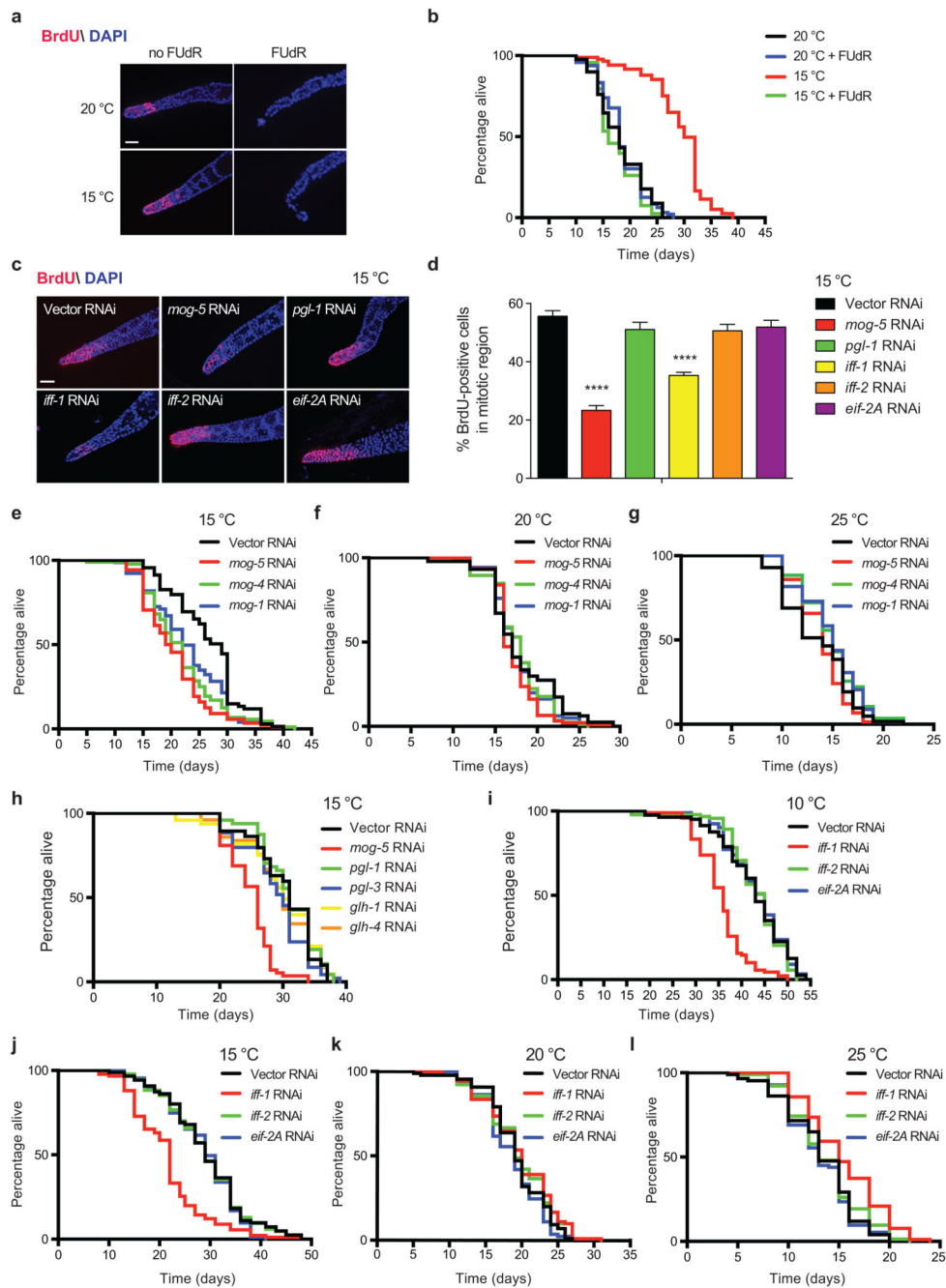


Figure 4. Adult GSC proliferation determines cold-induced longevity.

a, BrdU staining of germ lines from wild-type worms treated with $100 \mu\text{g ml}^{-1}$ FUDR during adulthood at the indicated temperatures after development at 20°C . Worms were examined at day 5 of adulthood. Nuclei were stained with DAPI. Scale bar represents $20 \mu\text{m}$. The images are representative of 3 independent experiments. **b**, FUDR during adulthood does not affect lifespan at 20°C (20°C mean \pm s.e.m: 18.23 ± 0.49 , $20^\circ\text{C} + \text{FUDR}$: 18.28 ± 0.40 , $P = 0.8617$), but reduces cold-induced longevity (15°C : 29.08 ± 0.60 , $15^\circ\text{C} + \text{FUDR}$: 17.49 ± 0.40 , $P < 0.0001$). **c**, BrdU staining of germ lines from wild-type worms examined at day 5 of

adulthood. Scale bar represents 20 μm . The images are representative of 3 independent experiments. **d**, Percentage of BrdU-positive cells/total nuclei (mean \pm s.e.m., Vector/*mog-5/iff-1* RNAi (n= 33 germ lines), *pgl-1/iff-2/eif-2A* RNAi (n= 36), germ lines from 3 independent experiments). Analysis by two-tailed Student's t-test for unpaired samples (**** (P<0.0001)). **e**, Knockdown of *mog* genes shortens cold-induced longevity (15°C) in wild-type worms. Vector RNAi mean \pm s.e.m: 26.60 \pm 0.74, *mog-5*: 20.52 \pm 0.63 (P<0.0001); *mog-4*: 21.83 \pm 0.69 (P<0.0001); *mog-1*: 22.87 \pm 0.76 (P= 0.0020). **f**, *mog* RNAi does not reduce lifespan of wild-type worms at 20°C. Vector RNAi mean \pm s.e.m: 17.96 \pm 0.46, *mog-5*: 17.13 \pm 0.28 (P= 0.0653), *mog-4*: 17.68 \pm 0.34 (P= 0.3608), *mog-1*: 17.58 \pm 0.34 (P= 0.2567). **g**, *mog* RNAi does not shorten lifespan of wild-type worms at 25°C. Vector RNAi mean \pm s.e.m: 13.50 \pm 0.42, *mog-5*: 13.93 \pm 0.27 (P= 0.7344), *mog-4*: 14.88 \pm 0.27 (P= 0.0420), *mog-1*: 14.76 \pm 0.36 (P= 0.0685). **h**, Knockdown of *pgl* and *glh* genes does not suppress cold-induced longevity in wild-type worms. Vector RNAi mean \pm s.e.m: 30.35 \pm 0.85, *mog-5*: 24.92 \pm 0.44 (P<0.0001), *pgl-1*: 30.96 \pm 0.65 (P= 0.6424), *pgl-3*: 28.95 \pm 0.72 (P= 0.2590), *glh-1*: 29.64 \pm 0.94 (P= 0.9853), *glh-4*: 29.57 \pm 0.81 (P= 0.7474). **i**, Loss of *iff-1* shortens cold-induced longevity in wild-type worms at 10°C. Vector RNAi mean \pm s.e.m: 42.45 \pm 0.84, *iff-1*: 35.52 \pm 0.54 (P<0.0001), *iff-2*: 43.00 \pm 0.66 (P= 0.6186), *eif-2A*: 43.11 \pm 0.68 (P= 0.8526). **j**, *iff-1* RNAi reduces cold-induced longevity in wild-type worms at 15°C. Vector RNAi mean \pm s.e.m: 29.19 \pm 0.86, *iff-1*: 21.66 \pm 0.76 (P<0.0001), *iff-2*: 29.24 \pm 0.85 (P= 0.8227), *eif-2A*: 28.53 \pm 0.74 (P= 0.3853). **k**, *iff-1* RNAi does not reduce lifespan at 20°C. Vector RNAi: mean \pm s.e.m: 19.33 \pm 0.45, *iff-1*: 19.79 \pm 0.51 (P= 0.1317), *iff-2*: 19.61 \pm 0.50 (P= 0.2137), *eif-2A*: 18.65 \pm 0.44 (P= 0.2061). **l**, *iff-1* RNAi induces a moderate lifespan extension at 25°C. Vector RNAi mean \pm s.e.m: 13.23 \pm 0.40, *iff-1*: 15.36 \pm 0.39 (P<0.0001), *iff-2*: 13.69 \pm 0.42 (P= 0.4603), *eif-2A*: 13.19 \pm 0.33 (P= 0.6935). In lifespan experiments, P-values: two-sided log-rank test, n= 96 worms/condition. RNAi initiated at day 1 of adulthood in all the experiments. Supplementary Data 3 contains replicate data of lifespan experiments.

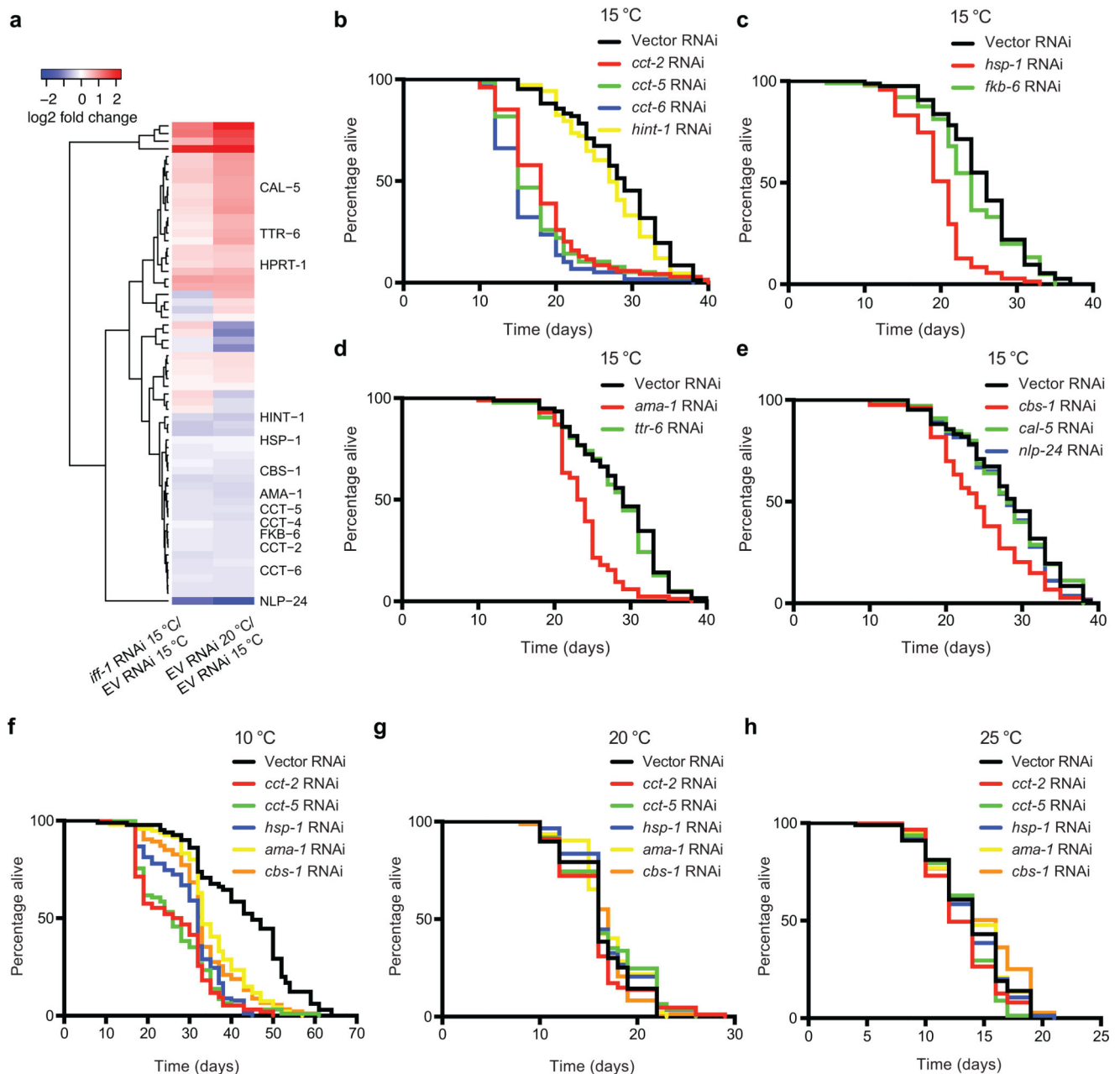


Figure 5. *cbs-1* and other factors modulate the long lifespan induced by adult GSCs at low temperatures.

a, Heatmap depicting the log₂-fold change of the differentially expressed proteins in both *iff-1* RNAi-treated worms at 15°C and empty vector (EV) RNAi-treated worms at 20°C when compared with EV RNAi-treated worms at 15°C. *fer-15(b26);fem-1(hc17)* control strain was raised at the restrictive temperature (25°C) during development to obtain sterile worms with a proliferating germline, which were then shifted to the indicated temperatures and RNAi treatment until day 6 of adulthood. Statistical comparisons were made by two-tailed Student's t-test ($n = 3$, p -value < 0.05 was considered significant). Lifespan experiments upon knockdown of the indicated proteins are presented in the following panels.

Supplementary Fig. 17 presents the heatmap with the full list of significantly changed proteins. For lifespan data of the other differentially expressed proteins, please see Supplementary Table 1. **b**, CCT subunits are required for cold-induced longevity (15°C) in wild-type worms (Empty vector RNAi mean \pm s.e.m: 28.26 ± 0.69 ; *cct-2* RNAi: 18.58 ± 0.71 , $P < 0.0001$; *cct-5* RNAi: 17.83 ± 0.68 , $P < 0.0001$; *cct-6* RNAi: 16.15 ± 0.66 , $P < 0.0001$; *hint-1* RNAi: 27.15 ± 0.69 , $P = 0.1722$). **c**, The *hsp-1* chaperone is necessary for cold-induced longevity (15°C) (Empty vector RNAi mean \pm s.e.m: 25.49 ± 0.62 ; *hsp-1* RNAi: 19.84 ± 0.49 , $P < 0.0001$; *fkf-6* RNAi: 24.10 ± 0.73 , $P = 0.2535$). **d**, The RNA polymerase II *ama-1* regulates longevity of wild-type worms at 15°C (Empty vector RNAi mean \pm s.e.m: 28.54 ± 0.68 ; *ama-1* RNAi: 23.67 ± 0.42 , $P < 0.0001$; *ttr-6* RNAi: 27.95 ± 0.65 , $P = 0.4734$). **e**, Loss of *cbs-1* decreases longevity of wild-type worms at 15°C (Empty vector RNAi mean \pm s.e.m: 28.26 ± 0.69 ; *cbs-1* RNAi: 24.54 ± 0.69 , $P = 0.0005$; *cal-5* RNAi: 28.09 ± 0.78 , $P = 0.8688$; *nlp-24* RNAi: 27.16 ± 0.78 , $P = 0.0664$). **f**, Knockdown of *cct* subunits, *hsp-1*, *ama-1* or *cbs-1* decreases the long lifespan phenotype induced by 10°C in wild-type worms ($P < 0.0001$). Empty vector RNAi mean \pm s.e.m: 43.31 ± 1.39 ; *cct-2* RNAi: 26.36 ± 0.02 ; *cct-5* RNAi: 26.76 ± 0.95 ; *hsp-1* RNAi: 30.17 ± 0.82 ; *ama-1* RNAi: 35.37 ± 0.87 ; *cbs-1* RNAi: 33.57 ± 0.93 . **g**, Knockdown of *cct* subunits, *hsp-1*, *ama-1*, or *cbs-1* does not shorten lifespan at 20°C. Empty vector RNAi mean \pm s.e.m: 16.34 ± 0.37 ; *cct-2* RNAi: median = 15.97 ± 0.41 , $P = 0.5386$; *cct-5* RNAi: 17.01 ± 0.48 , $P = 0.1106$; *hsp-1* RNAi: 17.10 ± 0.39 , $P = 0.1571$; *ama-1* RNAi: 17.02 ± 0.35 , $P = 0.4403$; *cbs-1* RNAi: 16.26 ± 0.43 , $P = 0.9592$. **h**, Knockdown of *cct* subunits, *hsp-1*, *ama-1*, or *cbs-1* does not shorten lifespan at 25°C. RNAi was initiated at day 1 of adulthood. Empty vector RNAi mean \pm s.e.m: 13.95 ± 0.37 ; *cct-2* RNAi: 13.20 ± 0.31 , $P = 0.0695$; *cct-5* RNAi: 13.43 ± 0.29 , $P = 0.0472$; *hsp-1* RNAi: 13.83 ± 0.36 , $P = 0.7389$; *ama-1* RNAi: 14.07 ± 0.36 , $P = 0.8221$; *cbs-1* RNAi: 14.53 ± 0.44 , $P = 0.1069$. In all the lifespan experiments, RNAi was started at day 1 of adulthood (P-values: two-sided log-rank test, $n = 96$ worms/condition). See Supplementary Data 3 for statistical analysis and replicate data of lifespan experiments.

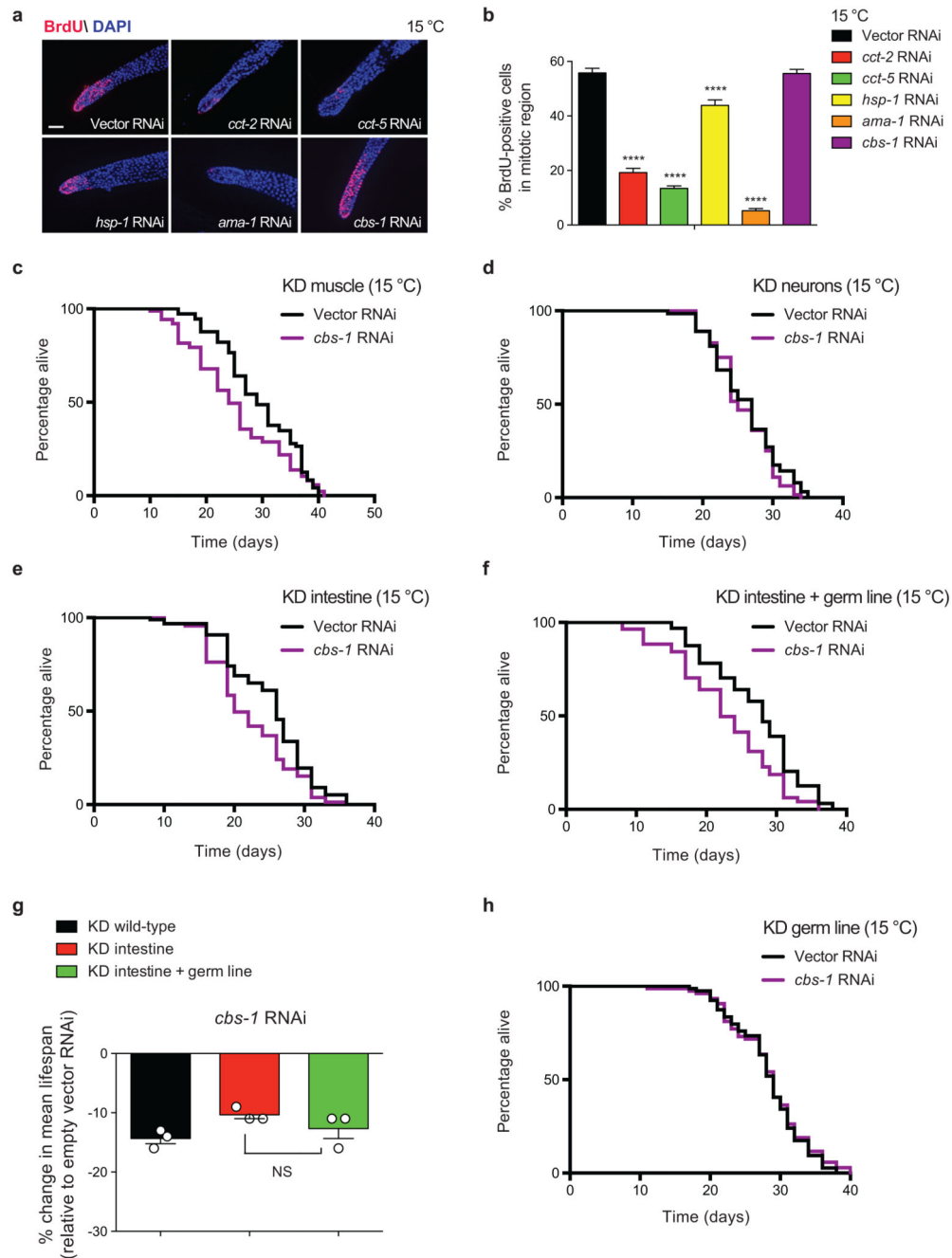


Figure 6. Tissue-specific knockdown of *cbs-1* in the intestine or muscle reduces cold-induced longevity.

a, BrdU staining of germ line from wild-type *C. elegans* fed with the indicated RNAi from day 1 of adulthood. Worms were examined at day 5 of adulthood. Cell nuclei were stained with DAPI. Scale bar represents 20 μ m. The images are representative of 3 independent experiments. **b**, Graph represents the percentage of BrdU-positive cells/total nuclei (mean \pm s.e.m., Vector, *cbs-1* RNAi (n= 46 germ lines), *cct-2*, *cct-5*, *hsp-1*, *ama-1* RNAi (n= 40), germ lines scored per each condition from 3 independent experiments). Statistical

comparisons were made by two-tailed Student's t-test for unpaired samples. P-value: **** (P<0.0001). **c**, Muscle-specific knockdown (KD) of *cbs-1* decreases lifespan extension induced by cold temperature (15°C). RNAi rescued in the muscle of RNAi-deficient worms (*rde-1(ne300); myo-3p::rde-1* strain). Empty vector RNAi mean \pm s.e.m: 29.49 \pm 0.81; *cbs-1* RNAi: 25.33 \pm 0.90, P=0.0048. **d**, Neuronal-specific KD of *cbs-1* does not affect longevity at 15°C. RNAi rescued in the neurons of RNAi-deficient worms (*sid-1(pk3321); unc-119p::sid-1* strain). Empty vector RNAi mean \pm s.e.m: 26.09 \pm 0.60; *cbs-1* RNAi: 25.78 \pm 0.51, P=0.3367. **e**, Intestinal-specific KD of *cbs-1* decreases longevity at 15°C. RNAi rescued in the intestine of RNAi-deficient worms (*rde-1(ne219); nhx-2p::rde-1* strain). Empty vector RNAi mean \pm s.e.m: 25.02 \pm 0.66; *cbs-1* RNAi: 22.25 \pm 0.65, P<0.0001. **f**, RNAi rescued in both the intestine and germ line of RNAi-deficient worms (*rde-1(ne219); mex-5p::rde-1* strain). Empty vector RNAi mean \pm s.e.m: 26.97 \pm 0.79; *cbs-1* RNAi: 22.72 \pm 1.00, P<0.0019. **g**, Percentage of mean lifespan change in different strains upon knockdown of *cbs-1* (relative to the respective empty vector RNAi control). Graph represents the mean \pm s.e.m. from 3 independent lifespan experiments for each strain. Longevity was not further reduced when both the intestine and the germ line responded to RNAi treatment when compared to knockdown in the intestine alone (KD intestine versus KD intestine + germ line, P= 0.2634). Statistical comparisons were made by two-tailed Student's t-test for unpaired samples. NS= not significant. **h**, Knockdown of *cbs-1* in the germ line alone does not decrease cold-induced longevity at 15°C. RNAi rescued in the germ line of RNAi-deficient worms (*rde-1(mkc36); sun-1p::rde-1::sun-1 3'UTR* strain). Empty vector RNAi mean \pm s.e.m: 28.32 \pm 0.55; *cbs-1* RNAi: 28.40 \pm 0.64, P=0.5733. In all the lifespan experiments, P-values: two-sided log-rank test, n= 96 worms/condition. RNAi was started at day 1 of adulthood. See Supplementary Data 3 for statistical analysis and replicate data of lifespan experiments.

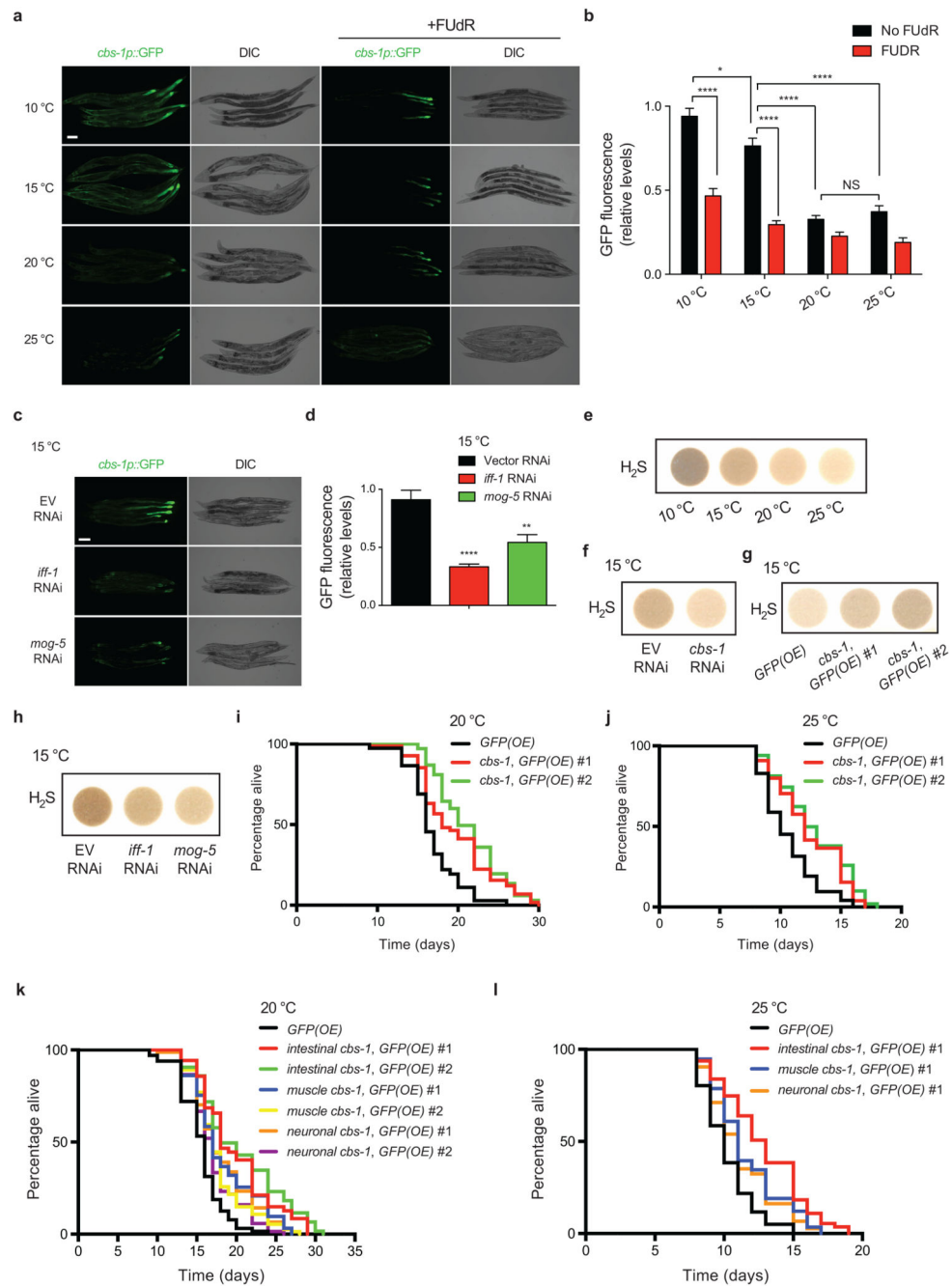


Figure 7. GSCs induce *cbs-1* expression in somatic tissues at cold temperature.

a, GFP expressed under *cbs-1* promoter in day 5 adult-worms grown at the indicated temperatures during adulthood. At 20°C and 25°C, *cbs-1* is mostly expressed in the posterior intestine. At cold temperatures, *cbs-1* expression increases in the intestine and muscle. FUDR reduces cold-induced expression of *cbs-1* in muscle and intestine. DIC, differential interference contrast. Scale bar, 100 μm. Images are representative of four independent experiments. **b**, Quantification of *cbs-1p::GFP* (mean ± s.e.m. relative to 10°C with no FUDR, 40 worms/condition from 4 independent experiments). Analysis by two-tailed

Student's t-test for unpaired samples: *($P < 0.05$), ****($P < 0.0001$). NS= not significant ($P = 0.2683$). **c**, *cbs-1p::GFP* in day 7 adult-worms at 15°C. Knockdown of either *iff-1* or *mog-5* during adulthood decreases *cbs-1* expression when compared to empty vector (EV) RNAi. Scale bar, 50 μ m. Images are representative of two independent experiments. **d**, Quantification of *cbs-1p::GFP* (mean \pm s.e.m. relative to EV RNAi, 20 worms/condition from 2 independent experiments). Analysis by two-tailed Student's t-test for unpaired samples: **($P < 0.01$), ****($P < 0.0001$). **e**, H₂S gas production in control sterile strain at day 6 of adulthood (*fer-15(b26);fem-1(hc17)*). Worms were raised at the restrictive temperature (25°C) and shifted to the indicated temperatures during adulthood. The images are representative of four independent experiments. **f**, H₂S production in day 6-adult control sterile worms upon knockdown of *cbs-1* during adulthood. The images are representative of four independent experiments. **g**, Somatic overexpression (OE) of *cbs-1* increases H₂S production. Two independent *cbs-1(OE)* lines were tested. The images are representative of two independent experiments. **h**, Loss of either *iff-1* or *mog-5* during adulthood decreases H₂S production. Control sterile worms at day 6 of adulthood were examined. The images are representative of three independent experiments. **i**, Ubiquitous somatic overexpression of *cbs-1* under *sur-5* promoter extends lifespan at 20°C ($P < 0.0001$). *GFP(OE)* mean \pm s.e.m: 16.83 \pm 0.36; *cbs-1,GFP(OE)* #1: 19.65 \pm 0.59; *cbs-1,GFP(OE)* #2: 21.28 \pm 0.49. **j**, Ubiquitous somatic *cbs-1(OE)* extends lifespan at 25°C ($P < 0.0001$). *GFP(OE)*: 10.61 \pm 0.26; *cbs-1,GFP(OE)* #1: 12.33 \pm 0.35; *cbs-1,GFP(OE)* #2: 12.75 \pm 0.38. **k**, Tissue-specific overexpression of *cbs-1* in the intestine (*gly-19p*), muscle (*myo-3p*) or neurons (*rgef-1p*) extends lifespan at 20°C ($P < 0.0001$). Intestinal-specific OE induced longer longevity compared with muscle or neuronal overexpression ($P < 0.01$). *GFP(OE)*: 15.56 \pm 0.34; intestinal *cbs-1,GFP(OE)* #1: 19.82 \pm 0.59; intestinal *cbs-1,GFP(OE)* #2: 20.47 \pm 0.66; muscle *cbs-1,GFP(OE)* #1: 18.31 \pm 0.51; muscle *cbs-1,GFP(OE)* #2: 17.73 \pm 0.40; neuronal *cbs-1,GFP(OE)* #1: 18.11 \pm 0.44; neuronal *cbs-1,GFP(OE)* #2: 17.17 \pm 0.36. Two independent tissue-specific *cbs-1(OE)* lines were tested for each tissue. **l**, Tissue-specific overexpression of *cbs-1* in the intestine ($P < 0.0001$), muscle ($P = 0.0002$) or neurons ($P = 0.0034$) extends lifespan at 25°C. Intestinal-specific OE induced longer lifespan compared with muscle ($P = 0.0142$) or neuronal ($P = 0.0008$) overexpression. *GFP(OE)* mean \pm s.e.m: 10.24 \pm 0.24; intestinal *cbs-1,GFP(OE)* #1: 12.82 \pm 0.36; muscle *cbs-1,GFP(OE)* #1: 11.62 \pm 0.28; neuronal *cbs-1,GFP(OE)* #1: 11.25 \pm 0.28. In lifespan experiments, comparisons were made by two-sided log-rank test, n= 96 worms/condition. Supplementary Data 3 contains replicate data of lifespan experiments.

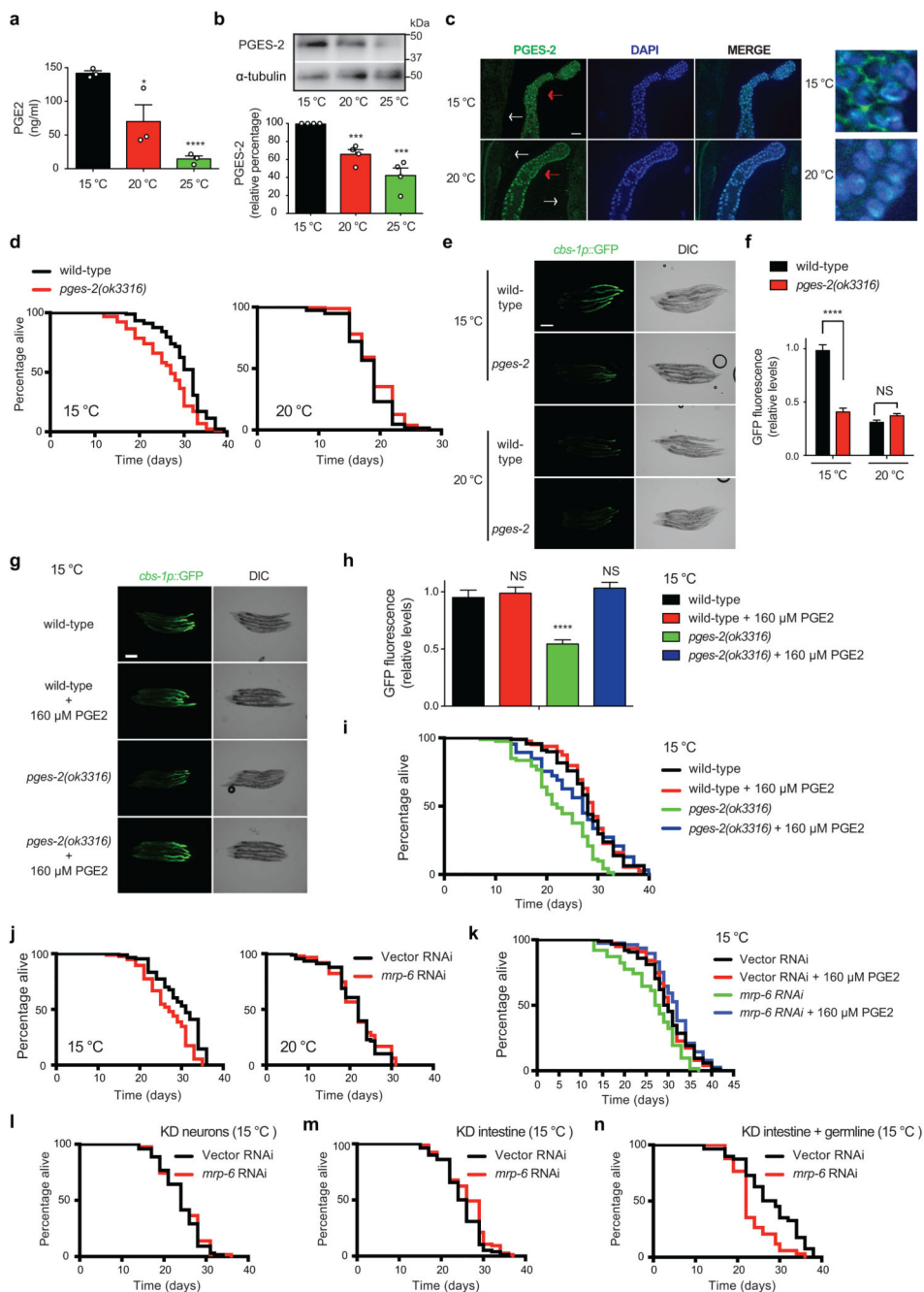


Figure 8. Release of PGE2 by GSCs promotes cold-induced longevity.

a, PGE2 levels in *fer-15;fem-1* control sterile worms at day 6 of adulthood (8.4 mg worms/ml, mean \pm s.e.m. from 3 independent experiments). Two-tailed Student's t-test for unpaired samples: * ($P < 0.05$), **** ($P < 0.0001$), NS = not significant ($P = 0.0519$). **b**, Western blot of day 6-adult control sterile worms with antibodies to PGES-2 and α -tubulin loading control. The graph represents PGES-2 relative percentage values (corrected for α -tubulin) to 15 °C (mean \pm s.e.m., 4 independent experiments). Two-tailed Student's t-test for unpaired samples: *** ($P < 0.001$). **c**, Immunostaining with PGES-2 antibody. White and red arrows

indicate intestine and germ line of day 6-adult wild-type worms, respectively. On the right, higher magnification of germ cells. Nuclei stained with DAPI. Scale bar, 20 μm . Images representative of three independent experiments. **d**, *pges-2(ok3316)* are short lived at cold temperature compared with wild-type animals (*pges-2* 15°C mean \pm s.e.m: 30.10 ± 0.52 , wild-type 15°C: 26.09 ± 0.66 , $P < 0.0001$), but do not live shorter at 20°C (*pges-2* 20°C: 18.13 ± 0.41 , wild-type 20°C 19.11 ± 0.37 , $P = 0.1303$). **e**, *cbs-1p::GFP* in adult wild-type and *pges-2(ok3316)* mutant worms (day 5). DIC, differential interference contrast. Scale bar, 1000 μm . Images representative of three independent experiments. **f**, Quantification of *cbs-1p::GFP* in day 5-adult animals (mean \pm s.e.m. relative to 15°C wild-type worms, 30 worms/condition from 3 independent experiments). Student's t-test for unpaired samples: ****($P < 0.0001$), NS ($P = 0.0519$). **g**, *cbs-1p::GFP* in day 8 adult-worms at 15°C. Exogenous PGE2 rescues low expression of *cbs-1* in *pges-2(ok3316)* mutants. Scale bar, 200 μm . Images representative of two independent experiments. **h**, Quantification of *cbs-1p::GFP* in day 8-adult animals at 15°C (mean \pm s.e.m. relative to non-treated wild-type worms. Wild-type ($n = 12$) and *pges-2* ($n = 15$) from 2 independent experiments). Two-tailed Student's t-test for unpaired samples: ****($P < 0.0001$), NS= wild-type versus wild-type + PGE2 ($P = 0.6614$), wild-type versus *pges-2* + PGE2 ($P = 0.4073$). **i**, Exogenous PGE2 extends the short lifespan of *pges-2(ok3316)* mutants at 15°C (*pges-2* versus *pges-2* + PGE2, $P < 0.0001$). Wild-type mean \pm s.e.m: 28.07 ± 0.59 ; wild-type + PGE2: 28.60 ± 0.58 ; *pges-2*: 22.43 ± 0.73 ; *pges-2* + PGE2: 26.54 ± 0.95 . **j**, *mrp-6* RNAi decreases lifespan of wild-type worms at 15°C (Vector RNAi mean \pm s.e.m: 29.64 ± 0.59 ; *mrp-6*: 26.66 ± 0.61 , $P < 0.0001$), but not at 20°C (Vector: 21.23 ± 0.58 ; *mrp-6*: 21.58 ± 0.64 , $P = 0.3707$). RNAi was initiated during adulthood. **k**, Exogenous PGE2 does not prolong cold-induced longevity of control worms (Vector RNAi mean \pm s.e.m: 29.85 ± 0.61 versus Vector + PGE2: 29.98 ± 0.59 , $P = 0.9106$), but extends the short lifespan of *mrp-6* RNAi-treated worms (*mrp-6*: 26.37 ± 0.82 versus *mrp-6* + PGE2: 31.43 ± 0.60 , $P < 0.0001$). **l**, Neuronal-specific *mrp-6* RNAi (Vector RNAi: 23.87 ± 0.56 , *mrp-6*: 24.18 ± 0.61 , $P = 0.5119$). **m**, Intestinal-specific *mrp-6* RNAi (Vector RNAi: 24.86 ± 0.51 , *mrp-6*: 26.16 ± 0.57 , $P = 0.0531$). **n**, When the germ line is sensitive to RNAi, *mrp-6* RNAi reduces cold-induced longevity (Vector RNAi: 27.77 ± 1.03 ; *mrp-6*: 23.32 ± 0.78 , $P = 0.0007$). Lifespan experiments were analyzed by two-sided log-rank test, $n = 96$ worms/condition. Supplementary Data 3 contains replicate lifespan experiments.

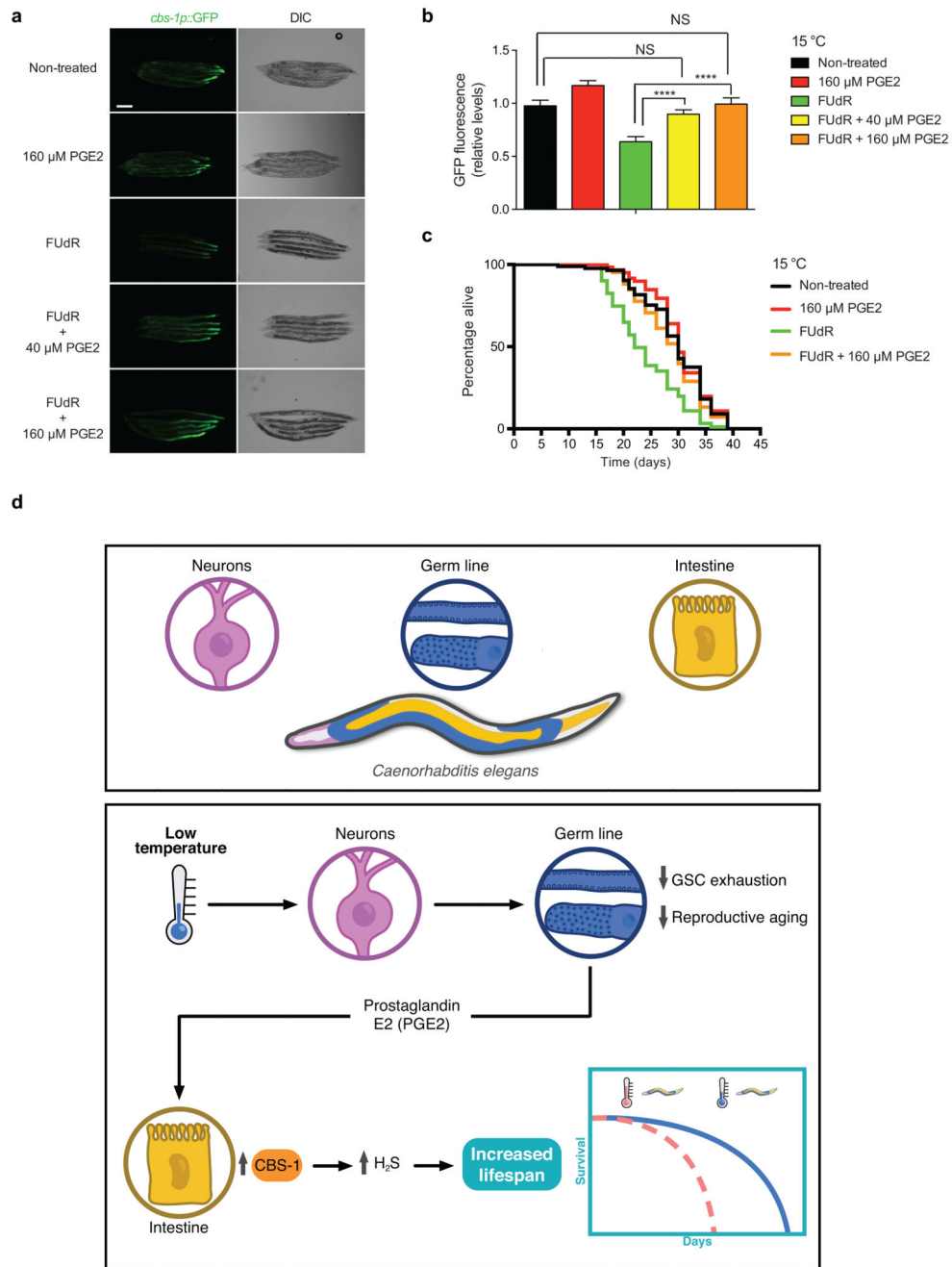


Figure 9. Application of exogenous PGE₂ rescues *cbs-1* expression and cold-induced longevity in GSC-impaired worms.

a, Representative images of GFP expressed under control of the *cbs-1* promoter in day 8 adult-worms at 15°C. Application of exogenous PGE₂ rescues low expression of *cbs-1* caused by FudR treatment (100 μg ml⁻¹). PGE₂ was added from day 5 of adulthood. DIC, differential interference contrast. Scale bar represents 200 μm. Images are representative of three independent experiments. **b**, Quantification of *cbs-1p::GFP* expression in day 8-adult animals at 15°C. Graph represents the mean ± s.e.m. relative to non-treated worms (Non-treated, PGE₂, FudR (n=50), FudR + PGE₂ (n=65), worms were analyzed per each

condition from three independent experiments). Statistical comparisons were made by Student's t-test for unpaired samples. P-value: ****($P < 0.0001$), NS (not significant): Non-treated versus FUdR+40 μM PGE2 ($P = 0.2436$), Non-treated vs FUdR+160 μM PGE2 ($P = 0.8706$). **c**, FUdR treatment reduces lifespan of wild-type worms at cold temperature (Non-treated versus FUdR, $P < 0.0001$), a phenotype rescued by application of exogenous PGE2 (PGE2 + FUdR versus FUdR, $P < 0.0001$). Non-treated mean \pm s.e.m: 29.30 ± 0.69 ; PGE2: 30.39 ± 0.70 , FUdR: 22.98 ± 0.63 , FUdR + PGE2: 28.38 ± 0.64 . P-values: two-sided log-rank test, $n = 96$ worms/condition. See Supplementary Data 3 for statistical analysis and replicate data of lifespan experiments. **d**, Model of cell-non-autonomous communication between somatic tissues and germ line at cold temperature. Somatic tissues such as IL1 and AFD neurons detect low temperature and ameliorate adult GSC exhaustion, which in turns delays reproductive aging. Adult GSCs release PGE2 hormone to induce *cbs-1* expression in the intestine, resulting in higher somatic production of pro-longevity H_2S gas. The rewiring of somatic tissues by GSCs extends organismal lifespan. This process coordinates extended reproductive capacity with long lifespan at cold temperature.